Chemical Science

ROYAL SOCIETY OF CHEMISTRY

REVIEW

View Article Online
View Journal | View Issue

Cite this: *Chem. Sci.*, 2026, **17**, 5331

Flexoelectric catalysis: mechanisms, material designs, and synergistic strategies

Yucheng Zhang, Tingfang Tian* and Linfeng Fei*

The emergence of the flexoelectric effect (*i.e.*, the linear electromechanical coupling between strain gradient and charge polarization) in a wide range of materials suggests a new catalytic mechanism in mechanocatalysis for activating chemical bonds and reactions. This review comprehensively summarizes the recent developments of flexoelectric catalysis, including its theoretical foundations, experimental breakthroughs, and advanced materials. It commences with the brief history and underlying mechanisms of flexoelectricity and flexoelectric catalysis. Then, the recent strategies for improving the performance of flexoelectric catalysts are reviewed. Subsequently, multi-field coupling strategies that can be used to achieve superior performance are discussed. Finally, the prevailing technical challenges together with the future directions are outlined, positing that flexoelectric catalysis is poised to bridge fundamental materials science with scalable clean energy solutions.

Received 15th November 2025
Accepted 10th February 2026

DOI: 10.1039/d5sc08929h

rsc.li/chemical-science

1. Introduction

Heterogeneous catalysis now plays a crucial role in diverse energy and environmental applications, typically involving solid catalysts that provide high catalytic activity, good selectivity, and long-term stability due to their large surface area and rich active sites.[1,2] However, it is notable that state-of-the-art catalysts usually showcase relatively low energy efficiency and always include precious metals (Pt, Pd, *etc.*) as essential constituents; driven by these issues, scientists are striving to pursue new catalytic mechanisms as well as novel catalysts.[3] Photocatalysis, for instance, leverages light to generate electron–hole pairs from photocatalysts, yet its efficiency is often constrained by their rapid recombination.[4,5] In recent years, apart from photocatalysis, the attractive ability of materials for using abundant and ubiquitous mechanical energy to catalyze chemical reactions (*i.e.*, mechanocatalysis) has emerged as a compelling alternative.[6,7] Piezocatalysis, a representative form of mechanocatalysis, promotes redox reactions directly *via* the polarization charges generated by the well-known piezoelectric effect (the electromechanical coupling between strain and polarization) in non-centrosymmetric materials under external stress.[8,9] However, due to the limited number of piezoelectric catalysts that possess high piezoelectric coefficients and sustain large strains, the development of piezocatalysis is far from satisfying, which has thereby initiated the research interest for other possible pathways in mechanocatalysis.[10,11]

School of Physics and Materials Science, Jiangxi Provincial Key Laboratory of Photodetectors, Jiangxi Engineering Laboratory for Advanced Functional Thin Films, Nanchang University, Nanchang, Jiangxi 330031, China. E-mail: feilinfeng@gmail.com; tftian@ncu.edu.cn

Yucheng Zhang

Yucheng Zhang is currently a PhD candidate in Prof. Linfeng Fei's group in the School of Physics and Materials Science, Nanchang University. His research interests include the controllable synthesis of nanocatalysts and their multi-field coupled catalysis.

Tingfang Tian

Tingfang Tian received her B.S. and Ph.D. degrees in materials science from the University of Science and Technology of China, followed by postdoctoral research at the University of South Carolina, USA. She is currently an associate professor in the School of Physics and Materials Science, Nanchang University. Her research mainly focuses on the development of photoelectrocatalysts and perovskite quantum dot luminescent materials/devices.

The flexoelectric effect is another kind of electromechanical coupling observed in materials under nonuniform deformations, entailing a coupling between electric polarization and strain gradients to induce piezoelectric-like polarization charges.[12] And in particular, compared to the piezoelectric effect that is exclusively available in non-centrosymmetric dielectrics, this phenomenon even widely exists in centrosymmetric materials, amorphous materials, and polymers (including insulators, semiconductors, liquid crystals, biological samples, *etc.*).[13–16] More critically, the strength of this effect is governed by the strain gradient in materials, which can be intrinsically amplified at reduced dimensions, making flexoelectricity a dominant and scalable mechanism in nanomaterials.[17] These fundamental characteristics of flexoelectric materials (universality and size-dependence) impart preferred potential of harvesting and transforming mechanical energy from environmental vibrations, such as wind and waves, into polarization charges to catalyze chemical reactions.[18] Therefore, flexoelectricity introduces a new dimension to the design of mechanocatalysis (*i.e.*, flexoelectric catalysis): the catalytic activity can be engineered not only through chemical compositions as those in other catalysis mechanisms but also by physical structures that maximize strain gradients. Clearly, this paradigm shift expands the material range of flexoelectric catalysts and enables the efficient engineering of high mechano-responsive catalysts.[19]

Currently, the most important thing for the development of this new catalysis mechanism is the search for high-performance catalysts. In this context, a wide range of materials have been explored by recent studies, including oxides and their derivatives (TiO_2, $SrTiO_3$, $ZnAl_2O_4$, *etc.*),[20–22] two-dimensional (2D) materials (MoS_2, $MoSe_2$, *etc.*),[23] and halides ($MAPbI_3$, *etc.*),[24] and most of them have shown considerable potential in flexoelectric catalysis. Furthermore, it is demonstrated that the proper engineering of materials dimensions, metastructures, and defects can even improve the flexoelectric catalytic performance.[25] These advancements have led to the deployment of flexoelectric catalysis in a series of scenarios; for instance, scientists have successfully substantiated flexoelectric-driven hydrogen evolution reaction (HER),[26] oxygen evolution reaction (OER),[27] hydrogen peroxide (H_2O_2) production,[28] dye degradation and biomedical applications.[29–31] Moreover, the synergies of flexoelectric catalysis with other catalysis mechanisms (photocatalysis, piezocatalysis, *etc.*) unlock its significance in complex catalytic environments.[32,33] Despite the rapid progresses, to date, no comprehensive review regarding the material designs and synergistic strategies for flexoelectric catalysis is available. To the best of our knowledge, there are only relevant papers that focus on either fundamentals of flexoelectricity or broader topics such as mechanocatalysis.[19,25] In this context, we provide the first systematic review for flexoelectric catalysis concerning the structure–property–mechanism frameworks, which may thereby benefit its development toward the common goals of decarbonize energy systems and carbon neutrality.

In this review, a comprehensive overview of this rising field is provided. First, the brief history and the fundamentals of flexoelectricity and flexoelectric catalysis are summarized. Subsequently, the advanced strategies for enhancing the flexoelectric response and catalytic efficiency through structure, interface, and strain gradient engineering of flexoelectric catalysts are reviewed. Notably, the coupling mechanisms of flexoelectric catalysis with other catalysis technologies (photo/piezocatalysis) are also discussed, showing the potential of synergistic applications. Finally, the technical challenges and future trends in flexoelectric catalysis are suggested, aiming to guide the development of flexoelectric catalysis from laboratories toward practical industrial implementations.

Linfeng Fei

Linfeng Fei received his B.S. degree in chemistry from University of Science and Technology of China, followed by a Ph.D. degree in applied physics from The Hong Kong Polytechnic University. He is currently a professor in the School of Physics and Materials Science, Nanchang University. His research mainly focuses on the development and multiscale characterization of emerging materials.

2. Brief history and fundamentals of flexoelectricity and flexoelectric catalysis

Flexoelectricity, as a universal electromechanical coupling effect existing in a wide range of materials, has gradually developed into a multifaceted community integrating fundamental theory, property regulation and practical applications, with flexoelectric catalysis emerging as one of its most promising applications in recent years.[34,35] To systematically clarify the theoretical basis and development context of this field, this section first reviews the evolutionary process of flexoelectricity and flexoelectric catalysis from theoretical speculation to experimental verification and application exploration, and then elaborates on the intrinsic mechanism of flexoelectric catalysis based on the flexoelectric effect.

2.1 The development of flexoelectricity and flexoelectric catalysis

The important milestones in the development of flexoelectricity from theoretical explorations to functional applications are highlighted in Fig. 1. The flexoelectric effect in solids was first theoretically identified by Mashkevich and Tolpygo based on their studies of lattice dynamics in crystals.[36] In 1964, a phenomenological framework for the description of the effect was further proposed by Kogan *et al.*[37] Subsequently, Mindlin developed a continuum theory that provided a unified description of electro-mechanical interaction in both piezoelectric and non-piezoelectric materials.[38] The first microscopic

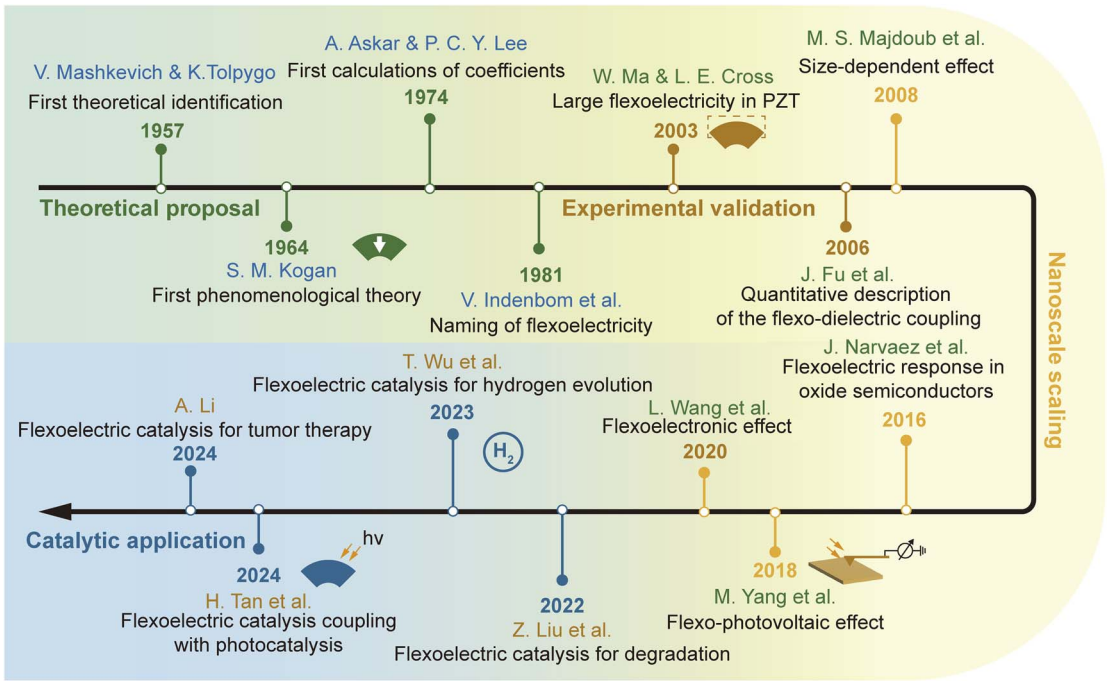

Fig. 1 Historical timeline of the major developments in the field of flexoelectricity and flexoelectric catalysis. Main stages, including theoretical proposal (1957–1981, initial theoretical identification and modeling), experimental validation (1974–2008, experimental verification of flexoelectric effects and coupling behaviors), nanoscale scaling (2006–2020, exploration of nanoscale flexoelectric phenomena), and catalytic application (2022–2024, demonstration of catalytic scenarios such as dye degradation, hydrogen evolution and tumor therapy), are outlined.

calculation of flexoelectric coefficients was performed by Askar *et al.* in 1974 in a number of simple crystals.[39] A decade later, Indenbom *et al.* first referred to the term "flexoelectricity" from liquid crystals, where an analogous phenomenon was thoroughly investigated.[40,41] Tagantsev *et al.* then indicated that flexoelectricity constitutes a fourth-order electro-elastic coupling that is more pronounced in materials with high dielectric constants.[42]

The development of this field underwent a shift in the early 21st century, moving from theoretical studies to experimental investigations of flexoelectric effects. Ma *et al.* revealed surprisingly high flexoelectric responses in soft lead zirconate titanate (PZT) perovskite ceramics.[43] In 2006, Fu *et al.* precisely measured the flexoelectric modulus in $Ba_{0.67}Sr_{0.33}TiO_3$, establishing a quantitative description of the flexo-dielectric coupling.[44] In theory, Majdoub *et al.* predicted the size dependence of the nanoscale flexoelectric effect in 2008: at a thickness of approximately 10 nm, the apparent piezoelectric coefficient induced by bending can reach 500% of that in the bulk phase, indicating that flexoelectricity is amplified in micro- and nanostructures.[45]

Over the past decade, relevant studies have focused on actively enhancing and coupling the flexoelectric effect in diverse materials. For instance, Narvaez *et al.* increased the effective flexoelectric coefficient of wide-bandgap oxide single crystals by orders of magnitude through doping to enhance their conductivity in 2016.[46] Subsequently, the coupling between flexoelectricity and photo/piezoelectirc effects was discovered.[47] For example, the photo-flexoelectric effect indicated that illumination can enhance or regulate the flexoelectric polarization charges.[47,48] In 2020, Wang *et al.* reported a flexoelectronic mechanism in centrosymmetric semiconductors (Si, Ge, GaAs, *etc.*) and suggested that the local flexoelectric polarization can regulate the metal–semiconductor contact barrier.[49]

Founded on these fundamental breakthroughs, it is therefore suggested that the ubiquitous nature of the flexoelectric effect renders it exceptionally appealing for mechanically driven catalysis. Recent years have witnessed the rapid advances of flexoelectric catalysis: Liu *et al.* reported the first case on dye degradation driven by flexoelectricity, wherein $SrTiO_3$ nanoparticles (NPs) degrade dyes under mechanical stimuli.[50] In 2023, Wu *et al.* investigated the highly efficient hydrogen generation by centrosymmetric high-entropy oxide through flexoelectric catalysis.[51] Furthermore, Wu *et al.* systematically investigated the key factors governing flexocatalytic efficiency, including material morphology, adsorption capacity, mechanical vibration intensity, and temperature.[52] In the same year, Tan *et al.* reported a strategy for flexoelectric–photocatalytic coupling, wherein the introduction of flexoelectricity remarkably enhanced photocatalytic efficiency.[32] Li *et al.* then employed flexoelectric catalytic technology to decompose tumor interstitial fluid, generating oxygen and reactive oxygen species, thereby effectively mitigating interstitial fluid pressure.[53] In 2025, Pan *et al.* demonstrated that the enhancement of flexoelectric catalysis efficiency can be achieved by tuning the intrinsic magnetism of the catalyst.[28] In short, over the past few decades, flexoelectricity and its derived fields have achieved

considerable progress, from fundamental theory to application fields. In particular, its integration with catalytic applications provides extensive research opportunities.[54] These fundamental principles and catalytic applications thus form the core of this review.

2.2 Mechanism of flexoelectric catalysis

The fundamental driving force underlying flexoelectric catalysis is flexoelectricity, the microscopic origin of which lies in the strain gradient that can disrupt local inversion symmetry, generating an electrical polarization field, as described by eqn (1).[55]

$$P_i = \mu_{ijkl} \frac{\partial \varepsilon_{kl}}{\partial x_j} \quad (1)$$

where P_i stands for the flexoelectric polarization, μ_{ijkl} is the fourth-order flexoelectric tensor (flexoelectric coefficient), $\partial \varepsilon_{kl}$ is the elastic strain, and ∂x_j is the coordinate satisfying $\mu_{ijkl} = \mu_{ijlk}$.

The flexoelectric effect is a higher-order electromechanical coupling phenomenon that can occur in dielectric materials, semiconductors, *etc.*[56] When the materials undergo inhomogeneous deformation (from external stress, lattice mismatch, dynamic strain, *etc.*), the consequent strain gradient displaces ionic positions and redistributes electron densities, inducing a macroscopic polarization (Fig. 2).[57] The catalytic mechanism unfolds through the concerted action of this polarization: (1) *Energy band bending and charge separation*. The flexoelectric polarization field acts as an internal bias across the catalysts, which causes band tilting in the materials, drives the separation of free charge carriers (electron–hole pairs) and effectively suppresses their recombination.[30,58] (2) *Surface reaction activation*. The charge accumulation and altered surface potential driven by the internal electric field directly modulate catalytic activity. The electric field lowers the energy barriers for key steps, while the separated charges provide the driving force for the adsorption, activation, and subsequent dissociation of reaction intermediates.[19,59] (3) *Redox reaction*. The charge carriers are transported through the bulk structure to the catalyst surface to participate in redox reactions such as oxygen reduction and hydroxyl oxidation, and thus to generate reactive hydrogen free radicals and hydroxy radicals for various catalytic applications.[25]

Consequently, the strain gradient governs the catalytic processes not only by inducing bulk polarization but also by controlling the spatial distribution of charge carriers and the energetics at the surface. This fundamental mechanism, which unifies mechanical deformation with electronic control, establishes flexoelectric catalysis as a distinct paradigm.

3. Structural modifications of flexoelectric catalysts

Flexoelectric catalysis has rapidly evolved from theoretical predictions to experimental demonstrations and materials engineering.[60] Actually, the intrinsic flexoelectric response in many materials is often weak, limiting their catalytic performance. Consequently, the amplification of flexoelectric polarization emerges as a significant strategy for improving the performance of flexoelectric catalysis.[61,62] This is generally achieved by engineering the material's structure across multiscales to generate and amplify the fundamental driving force (*i.e.*, the internal strain gradient) for charge production.[46,63] The magnitude of this gradient is inversely proportional to the characteristic dimensions of flexoelectric catalysts, making nanoscale design a foundational imperative.[49,64] This section thereby reviews the principal structural modification strategies, which are categorized into three interconnected approaches across different scales: (1) geometric structure design at the nano- and micro-scale, which leverages the shape of catalysts to concentrate strain under mechanical load (Fig. 3a); (2) interface engineering, which creates internal strain gradients through

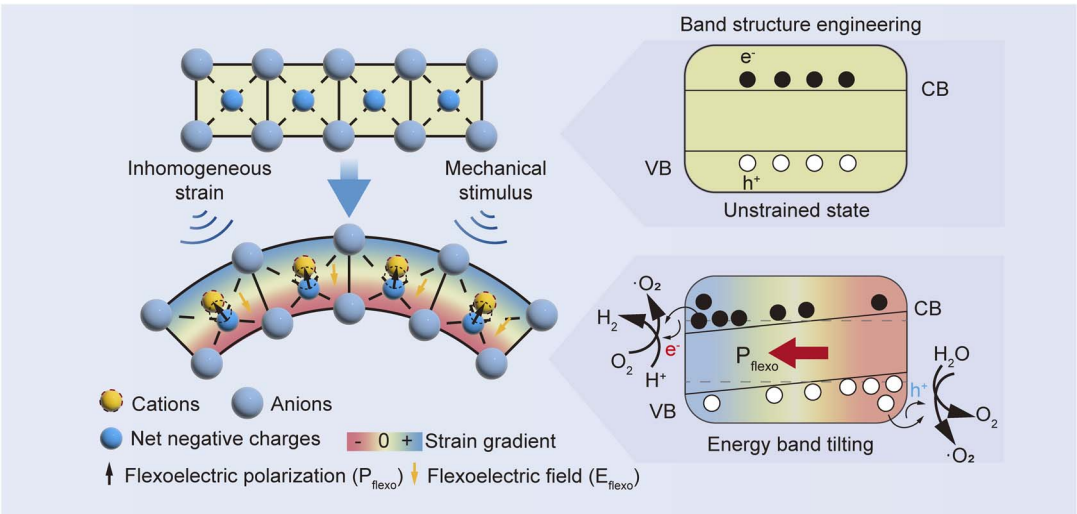

Fig. 2 Mechanism of flexoelectric catalysis.

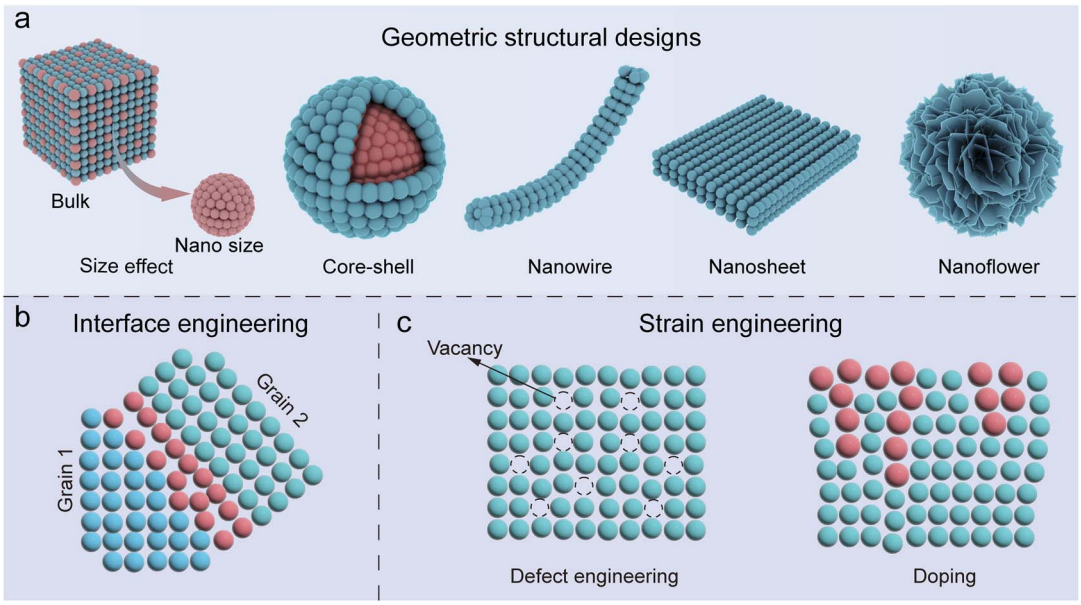

Fig. 3 Schematic diagram for structural modifications of flexoelectric catalysts. (a) Geometric structural designs, (b) interface engineering, and (c) strain engineering.

heterojunctions and boundaries (Fig. 3b); and (3) strain engineering at the atomic scale, which introduces localized lattice distortion through doping and defects (Fig. 3c). In short, these modifications enhance the strain gradient to significantly improve the flexoelectric response, thereby boosting catalytic efficiency for flexoelectric catalysts.

3.1 Geometric structural designs

Geometric structural design serves as the most direct method to amplify strain gradients by engineering the catalyst's morphology. The fundamental objective is to engineer structures that effectively amplify the intrinsic strain gradient under mechanical load.[65,66] Reducing the size of flexoelectric catalysts to the nanoscale is a fundamental strategy, as the strain gradient scales inversely with the characteristic dimension, significantly amplifying flexoelectric polarization.[67–69]

Du *et al.* systematically compared the catalytic performance of TiO_2 (rutile) NPs and reported that reducing the particle size from 300 nm to 50 nm increases the H_2 production rate from 1390 to 2380 μmol g^{-1} h^{-1}. This enhancement is clarified by a two-dimensional model illustrating the dependence of oriented strain gradients on particle size (Fig. 4a).[20] A similar result regarding the size-dependent effect is reflected in the work of Mondal *et al.*[21]

On the basis of size effects, geometry structural designs can further optimize the flexoelectric response.[71–73] Both theoretical and simulation studies have demonstrated that nanostructures such as NPs, one-dimensional (1D) nanorods (NRs)/nanowires (NWs), 2D nanosheets (NSs), and nanoflowers can exhibit high flexoelectric responses under similar mechanical stimuli.[52,74–76] This provides crucial mechanistic support for achieving efficient energy conversion and catalytic performance *via* structural engineering.

Han *et al.* construct hydroxyapatite@fluorapatite (HAP@FAP) core–shell NRs to enhance the flexoelectric response *via* structural design of flexoelectric catalysts (Fig. 4b).[70] The induced lattice strain at the core–shell interface creates an internal strain gradient, which triggers a robust flexoelectric polarization. Under ultrasonic excitation, the coupling effect between the flexoelectric field and the piezoelectric effect of HAP generates charge separation and enhances catalytic activity.

In the authors' previous study, the catalytic performance of 1D $MAPbI_3$ NWs is compared with that of NPs under equivalent mechanical stress. The reduction in dimensional scale grants nanostructures exceptional flexibility, enabling the NWs to sustain a larger strain gradient of 4×10^5 m^{-1} (Fig. 4c).[24] Consequently, the NWs deliver a stronger flexoelectric response and achieve a higher H_2 production rate (756.5 μmol g^{-1} h^{-1}). In addition, Sai *et al.* synthesize CeO_2 NRs that enable simultaneous dye degradation without compromising the H_2 evolution rate.[77] The flexoelectric polarization in a bending NR creates an internal electric field that promoted the separation of the thermal-excited electrons and holes.

In addition, hierarchical and layered structures provide further advantages for flexoelectric catalysis. Du *et al.* synthesized layered barium dititanate ($BaTi_2O_5$) nanocrystals, where alternating odd and even layers create internal polarization, resulting from strain gradient-induced symmetry disruption (Fig. 4d).[26] This inherent layered structure, which combines ferroelectric–flexoelectric responses, facilitates high H_2 evolution (1160 μmol g^{-1} h^{-1}) and dye degradation under ultrasound. In this case, the acoustic power from bubble cavitation generates a strain gradient that disrupts local symmetry, resulting in a non-equivalent flexoelectric polarization.

Wu *et al.* demonstrate that the dynamic flexoelectric polarization of ultrasonically stimulated nanoflower structures in

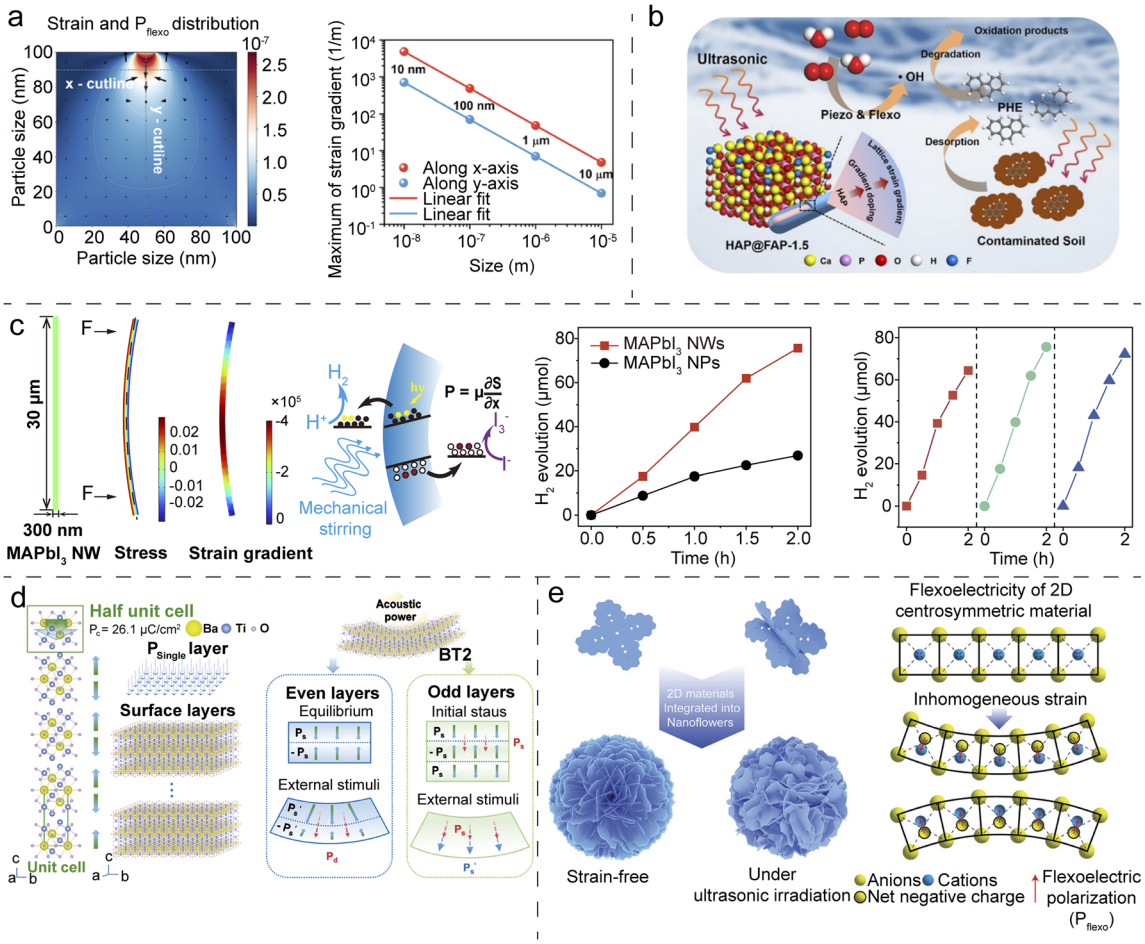

Fig. 4 Geometric structural designs. (a) 2D tip-force induced strain gradient and flexoelectric polarization distribution; relationship demonstration between rutile TiO_2 particle size and strain gradient variation by applying same amount of tip-force (10 μN m^{-1}) along the *z*-axis downwards.[20] Copyright 2024 Elsevier. (b) Schematic illustration of the proposed mechanism for flexo-piezocatalytic degradation by FAP@HAP core–shell NRs.[70] Copyright 2023 Royal Society of Chemistry. (c) Finite element method (FEM) results for bending-induced stress distribution within a single $MAPbI_3$ NW; time-dependent H_2 evolution profiles for $MAPbI_3$ NWs and NPs *via* photo-mechanical coupling; the test of stability for photo-mechanocatalytic H_2 evolution using $MAPbI_3$ NWs over three cycles.[24] Copyright 2024 Royal Society of Chemistry. (d) Theoretical calculation and structural illustration of polarization in single-layer $BaTi_2O_5$.[26] Copyright 2024 Wiley-VCH. (e) Schematic showing the nanoflower-like structure integrated with 2D NSs under strain-free conditions and ultrasonic irradiation.[52] Copyright 2023 Wiley-VCH.

centrosymmetric semiconductors (MnO_2 NSs) can sustainably promote redox reactions (Fig. 4e), effectively degrading organic pollutants with high efficiency, stability, and reproducibility.[52] Analytical calculations of the spatial strain distribution in individual NSs under uniform pressure reveal a strain gradient as large as 10^7 m^{-1}, which induces a pronounced out-of-plane flexoelectric polarization throughout the entire NS. These results demonstrate that a large strain gradient can be generated in the nanoflower integrated with NSs under ultrasonic irradiation, leading to effective internal flexoelectric polarization.

Therefore, the size effect and structural design have shown their potential for enhancing flexoelectric catalytic performance. The former amplifies strain gradients by reducing dimensions, while the latter optimizes local strain distribution *via* heterojunctions, wrinkled structures, or high-aspect-ratio structures. This combination expands the range of usable materials and provides new approaches to develop efficient, low-cost, and sustainable mechanically driven catalytic systems.

3.2 Interface engineering

Interface engineering represents a potent strategy to create built-in strain gradients that persist even in the absence of external stress.[63] Interfaces such as epitaxial films, heterojunctions and grain boundaries (GBs) can generate substantial, localized strain gradients due to local lattice mismatch and interfacial stress.[78–80] The strain gradients thus drives a static flexoelectric polarization, effectively creating a permanent internal electric field.[81] This field not only promotes the separation of charge carriers but also can be coupled with other interfacial features (such as heterojunction band alignments) to synergistically direct these charges toward catalytically active sites.

Recently, extensive studies have been conducted on interfaces and heterostructures for flexoelectric catalysis. For

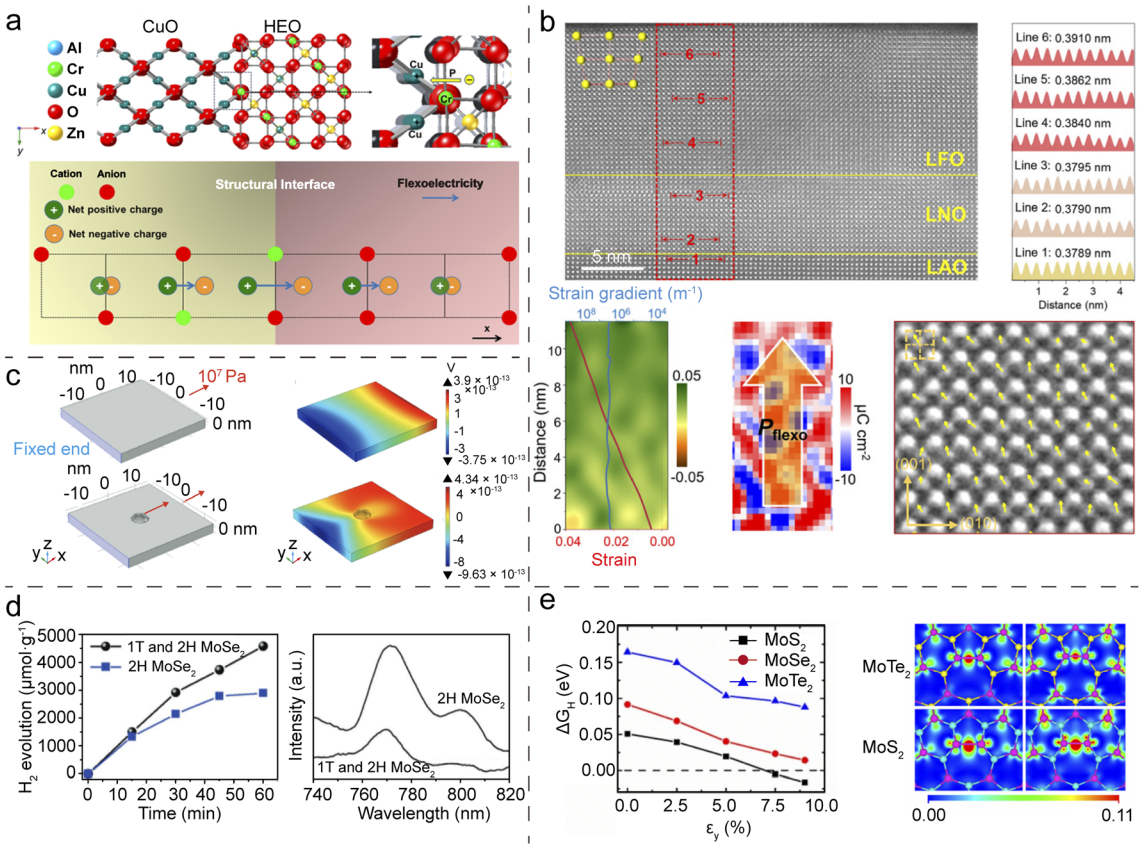

Fig. 5 Interface engineering. (a) Schematic illustration of phase discontinuity between $Ag(CuZn)(AlCr)_2O_4$ and CuO phases and flexoelectricity occurring at the structural interface.[51] (b) High-angle annular dark-field scanning transmission electron microscopy (HAADF-STEM) image of the LFO/LNO/LAO structure; in-plane lattice constants of the atom lines in the red box; in-plane strain e_{xx} images of the LFO layers by GPA analysis; distributions of electric polarizations in the LFO layers; mappings of Fe ion displacement vectors of the LFO layers.[27] Copyright 2024 AIP Publishing. (c) Simulation model for g-C_3N_4 and SA-Pt/CN NS; the corresponding simulation results of piezopotential.[83] Copyright 2024 Wiley-VCH. (d) Comparison of HER performance for the hybrid 1T- and 2H-phase and 2H-phase $MoSe_2$ nanoflowers; comparison of the intensity of photoluminescence for the corresponding catalysts.[23] Copyright 2020 Wiley-VCH. (e) Comparison of H_2 adsorption free energies ΔG_H after water dissociation for three catalysts; 2D projections of partial charge densities of the energy bands in the energy range from −0.15 to 0.15 eV for GB-containing $MoTe_2$ and MoS_2.[84] Copyright 2022 Springer Nature Link.

instance, Wu *et al.* constructed a hierarchically wrinkled $Ag(CuZn)(AlCr)_2O_4$/CuO high-entropy oxide nanocomposite (Fig. 5a).[51] The $Ag(CuZn)(AlCr)_2O_4$ and CuO phases exhibit centrosymmetric structures. At the structural boundaries, strain-induced lattice distortion causes a redistribution of mobile ions to generate deviation charges and produces flexoelectric polarization along the corresponding direction to balance the charges.[82] Therefore, a non-uniform flexoelectric field distribution across the spinel structure is established that suppresses electron–hole recombination. Under ultrasonic vibration (in the absence of light irradiation), this nanocomposite structure enables a high H_2 production rate of 2116 μmol g^{-1} h^{-1}.

In the field of thin-film heterostructures, Wang *et al.* reported remarkably enhanced OER activity in $LaFeO_3$ (LFO) thin-films *via* strain gradient-induced flexoelectric effects.[27] In the architecture, high-quality LFO catalyst layers and $LaNiO_3$ (LNO) electrode layers are epitaxially grown on a $LaAlO_3$ (LAO) substrate (Fig. 5b). Geometric phase analysis (GPA) quantifies gradual strain relaxation, revealing a massive strain gradient of 3.0×10^6 m^{-1} throughout the entire LFO layer, which produces a flexoelectric polarization field. In the catalytic situation, hydroxyl ion adsorption is strengthened on the polar LFO surface, and the electron transfer from the reactants and key intermediates to the catalyst across the band-tilted LFO layer is accelerated. These findings highlight the importance of the flexoelectric effect in OER kinetics.

The introduction of single-atom Pt into g-C_3N_4 (SA-Pt/CN) induces local lattice distortion and enhances strain gradients.[85] FEM simulations demonstrate that loaded Pt single atoms exhibit pinning effects under stress, generating significant strain gradients in the surrounding region (Fig. 5c). This effectively disrupts the symmetric structure, increases flexoelectric polarization, and thus improves the photo-mechanical coupled catalytic performance.

$MoSe_2$ NSs with mixed 1T/2H phase boundaries also exhibit strain-induced flexoelectric and piezoelectric polarization at their phase boundaries, producing a barrier-regulating effect.[23] This coupled polarization arises because the strain gradient, induced by bending the NSs, displaces Mo ions by

approximately δ_z along the z-axis, disrupting inversion symmetry. This significantly reduces electron–hole recombination and enhances H_2 production, achieving a rate of 4858.2 μmol g^{-1} h^{-1} (Fig. 5d).

Recent studies have further revealed the unique role of atomic-scale geometric configurations at GBs in the flexoelectric effect. Through first-principles calculations, in-plane tensile loading of single-layer transition metal dichalcogenides (TMDs) induces nonuniform deformation and strain gradients at GBs.[84] The enhanced local flexoelectric effect reduces the energy barriers associated with water splitting and hydrogen adsorption free energy at the GBs, significantly boosting the HER rate (Fig. 5e).

In all, interface engineering significantly enhances the flexoelectric effect by tailoring local symmetry disruption at various interfaces, including phase boundaries and GBs. The strain gradients introduced at these interfaces effectively retard electron/hole recombination and promote the generation of surface-active species while also promoting band restructuring. Besides, introducing flexoelectric polarization at GBs can substantially lower the energy barriers of key reaction steps.[51]

3.3 Strain engineering

Strain engineering at the atomic scale aims to introduce localized strain gradients through lattice mismatch such as chemical doping and the controlled introduction of vacancy defects, which disrupt the local crystal field symmetry.[86,87] When these perturbations are non-uniform (the concentration gradient of doping/non-homogeneous distribution of defects), they can generate internal strain gradients that induce a localized flexoelectric polarization.[88,89] These methods can effectively tune the surface electronic structure, accelerate charge carrier transport, and create highly active sites, thus enhancing the flexoelectric catalytic performance.[90,91]

Narvaez *et al.* discovered that semiconductor doping can significantly enhance the flexoelectric response by orders of magnitude (Fig. 6a).[46] For instance, oxygen-depleted $BaTiO_3$ ($BaTiO_{3-\delta}$) exhibits an effective flexoelectricity two orders of magnitude higher than that of insulating $BaTiO_3$, and Nb-doped TiO_2 yields a flexoelectric coefficient as high as 10^{-6}–10^{-5} C m^{-1}. Ma *et al.* observed that the effective flexoelectric response in Nb-doped $SrTiO_3$ (NSTO) single crystals increases with Nb-doping concentration and exhibits a linear relationship with the reciprocal of the depletion layer width.[92] Due to Nb doping, the sign of the flexoelectric-like effect is reversed, emphasizing the distinction from intrinsic flexoelectricity and providing a strategy for applying flexoelectricity at the macroscale (Fig. 6b).

Also building on this point, in the authors' previous work, high aspect-ratio F-doped hydroxyapatite NWs (F-HAP NWs) capable of generating significant nanoscale strain gradients under mechanical stimulation are synthesized for catalytic applications.[89] In addition, gradient doping with F ions induces lattice mismatch and localized strain, as shown in Fig. 6c. The coupling of nanoscale (*i.e.*, NW structure) and atomic-scale (*i.e.*, F doping) strain gradients induces a markedly enhanced flexoelectric response in F-HAP NWs, resulting in a H_2 generation rate of 322.7 μmol g^{-1} h^{-1} in pure water.

Oxygen vacancies (O_v) are among the most common and significant defect forms in oxide systems, with their concentration generally exerting a noteworthy influence on flexoelectric properties. Chen *et al.* employed defect engineering of O_v to enhance the flexoelectric effect in 2D TiO_2 NSs, effectively suppressing electron–hole recombination.[93] Density functional theory (DFT) calculation reveals stress-induced O_v formation, enabling spontaneously dissociation of water molecules on the surface of TiO_2 under dark conditions (Fig. 6d). Tu *et al.* optimized the flexoelectric catalytic performance of wide-bandgap spinel oxide $ZnAl_2O_4$ (ZAO) by tuning the O_v concentration.[22] The ZAO-200 sample (annealed at 200 °C) achieves an ultra-long carrier lifetime of 4.65 ns and an H_2 evolution rate of 3736.6 μmol g^{-1} h^{-1} (Fig. 6e).

The combination of defect engineering and wrinkle-induced strain presents a powerful synergistic strategy. Through first-principles calculations, Pu *et al.* identified that the catalytic activities of vacancy-defected TMD MX_2 monolayers for the HER can be significantly improved by wrinkle engineering (Fig. 6f and g).[94] The enhanced catalytic activity of TMDs is mainly attributed to the charge transfer and polarization enhancement of Mo atoms around the vacancy sites, which are caused by the wrinkling deformation and vacancy defect induced flexoelectricity.

As shown above, strain gradient engineering *via* doping and defects represents the most fundamental approach to implanting strain gradients directly at the atomic scale. Unlike geometric or interfacial strategies that often rely on external forces, this method creates internal, localized flexoelectric polarization fields that persistently modulate the surface electronic structure. This direct manipulation of the catalytic interface through lattice control not only enhances charge dynamics but also optimizes the adsorption behavior of intermediates, establishing a powerful design for high-performance flexoelectric catalysts.

3.4 Design principles of flexoelectric catalysts

Through above cases, one can be noted that the core design principle of flexoelectric catalysts is maximizing strain gradients *via* multiscale structural engineering to strengthen flexoelectric polarization and thereby catalytic efficiency. Geometric structure design leverages size effects and morphologies (*e.g.*, NPs, NWs, or nanoflowers) to enhance deformation capability of catalysts under mechanical stimuli. Interface engineering at the interfacial regions of heterojunctions, GBs, or phase boundaries facilitates a built-in strain gradient. The interfacial lattice mismatch may not only induce stable flexoelectric polarization and synergistically regulate charge separation, but also serve as active sites. Strain engineering introduces localized strain gradients through doping or defect engineering to modulate surface electronic structures and active sites. The optimization of a single factor cannot yield flexoelectric catalysts with exceptional performance, and thus the development of such catalysts requires the adoption of a multiscale design

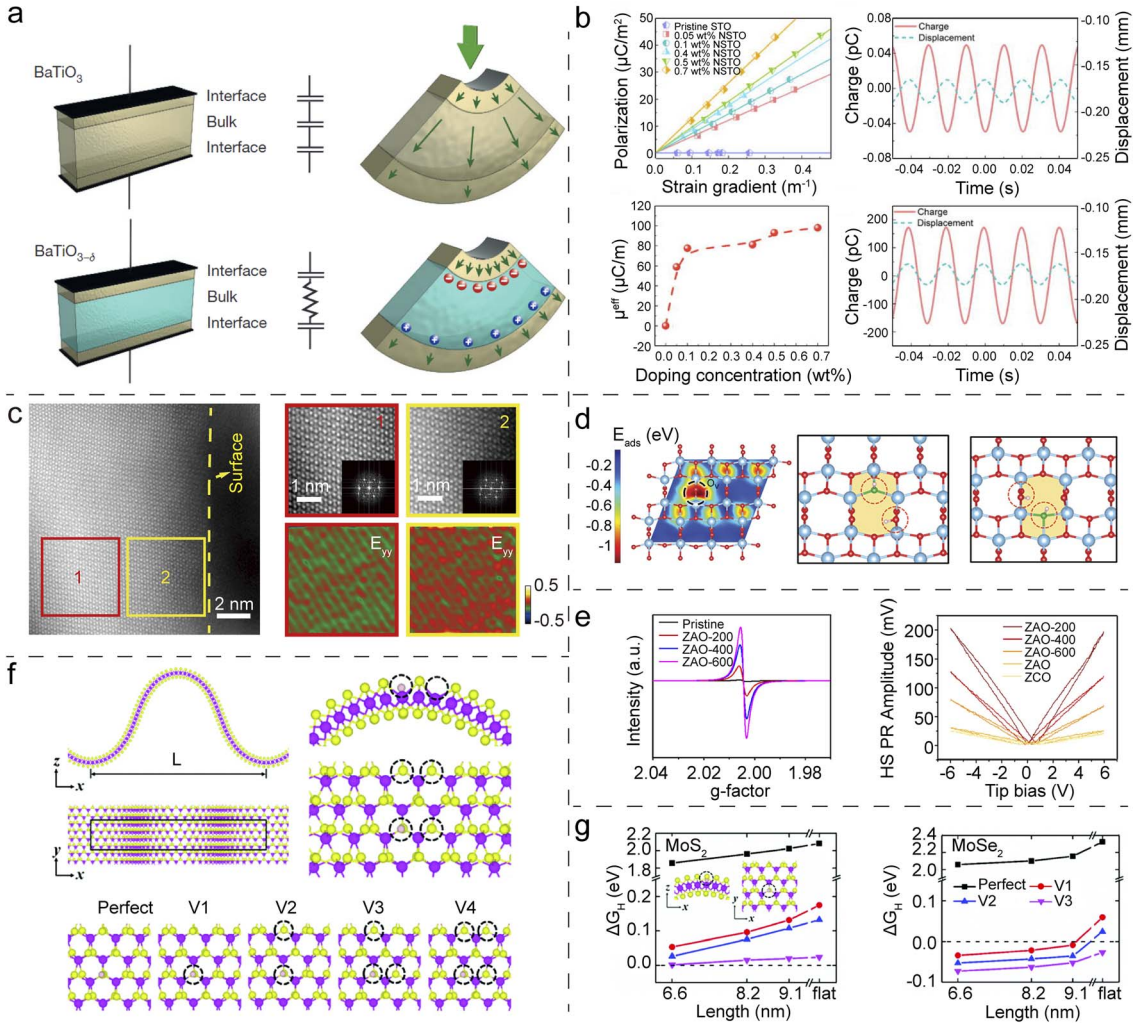

Fig. 6 Strain engineering. (a) Polar contributions from bulk flexoelectricity and surface piezoelectricity are present in its electromechanical response to bending; a semiconductor can form depletion layers at the interfaces with the electrodes; the conducting bulk acts as an intercalated electrode (blue layer) between interfacial barrier layers that respond as thin capacitors.[46] Copyright 2016 Springer Nature (b) Relationship between polarization and strain gradients in $SrTiO_3$ and NSTO single crystals with doping concentrations of 0.05, 0.1, 0.4, 0.5, and 0.7 wt%; the relationship between the effective flexoelectric coefficient and the Nb-doped concentration; the Fourier filtered first-harmonic displacement (the cyan curve) and charge (the red curve) for $SrTiO_3$ and 0.05 wt% NSTO.[92] Copyright 2023 AIP Publishing. (c) HAADF-STEM images and GPA analysis of F-HAP NWs, showing the strain gradients at the atomic level due to gradient F doping.[89] Copyright 2025 Royal Society of Chemistry. (d) Potential energy surface of H_2O adsorption on a defective TiO_2 surface with O_{V1}; strain-induced O_{V2} (defects are highlighted in yellow); O_{V3} endows water molecules with the ability to self-dissociate (the dashed circle indicates the product of the dissociation).[93] Copyright 2024 Wiley-VCH. (e) Electron paramagnetic resonance spectra of ZAO samples with various O_v concentrations; overlay of the piezoelectric force microscopy butterfly curve patterns of ZAO samples.[22] Copyright 2025 Wiley-VCH. (f) Side and top views of the relaxed structure of a wrinkled MoS_2 monolayer, the vacancy locations of the wrinkled MoS_2 monolayers, and the adsorption sites of the H atoms (the purple, yellow and white balls are Mo, S and H atoms, respectively; the dashed circles denote the vacancies where the S atoms are removed).[94] Copyright 2021 Royal Society of Chemistry. (g) Hydrogen adsorption Gibbs free energies (ΔG_H) of flat and wrinkled TMDs (MoS_2 and $MoSe_2$) with or without vacancies at different wrinkle lengths.[94] Copyright 2021 Royal Society of Chemistry.

approach to achieve the synergistic regulation and engineering optimization of multiple factors.

4 Hybrid coupling strategies of flexoelectric catalysis

The strategies outlined above focus on maximizing the intrinsic flexoelectric response of catalysts. However, the ultimate catalytic efficiency may still be constrained by fundamental limitations, such as finite charge carrier density or recombination losses.[95] It should therefore be noted that the inherent nature of flexoelectric polarization provides a unique opportunity to overcome these limits by coupling with other catalytic mechanisms. In such hybrid systems, the flexoelectric field does not merely add to other effects; it can directly modulate and synergize with the fundamental processes of other catalysis mechanisms (*e.g.*, photocatalysis and piezocatalysis), which lead to performance gains greater than the sum of the

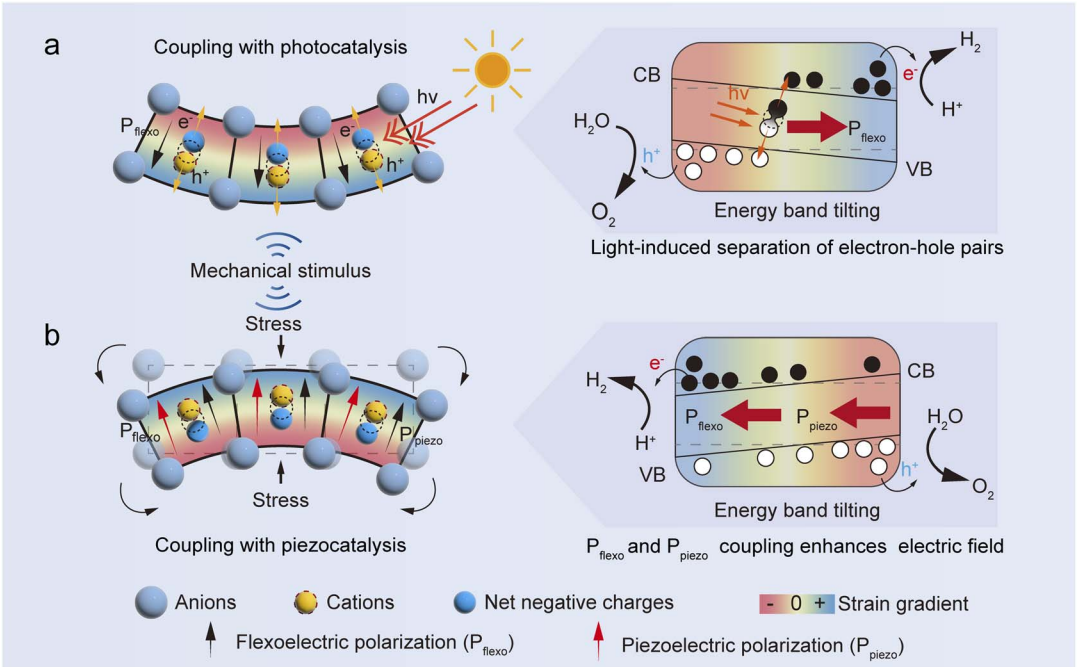

Fig. 7 Synergistic mechanism of flexocatalysis coupling with photo/piezocatalysis. (a) Flexo–photocatalysis. (b) flexo–piezocatalysis.

individual ones.[33] In this section, the recent advances in such coupling approaches are reviewed, with an emphasis on their core synergistic mechanisms.

4.1 Coupling with photocatalysis

The rapid recombination of photogenerated charge carriers and low quantum efficiency often plague photocatalytic processes.[96,97] The coupling of flexoelectricity with photocatalysis provides a new approach, termed "photo-mechanical" coupling, to drive catalytic reactions.[47,98] Under illumination, photogenerated electron–hole pairs undergo rapid separation. In this case, under mechanical stimuli, the induced flexoelectric polarization field superimposes on the intrinsic band structure of the semiconductor photocatalysts.[99] This not only provides an additional driving force for the separation of photogenerated electron–hole pairs but can also effectively guide their separation along a specific pathway, inhibit their rapid recombination, and achieve more efficient spatial charge separation.[24] Furthermore, this electric field can dynamically modulate the band tilting, thereby optimizing the process of catalytic reactions (Fig. 7a).[100] Meanwhile, flexoelectric polarization influences the adsorption and activation of key intermediates by altering the potential distribution on the surface of catalysts.[27,101]

Shao *et al.* discovered a ferroelastic twin texture in a centrosymmetric epitaxial $BiVO_4$ (BVO) film, where substantial strain gradients confined to the domain walls generate in-plane flexoelectric fields.[102] These fields at the boundaries spatially separate photogenerated charge carriers, driving electrons and holes toward opposite domains and thus facilitating the photocarrier transport. This flexo–phototronic mechanism is further corroborated by enhanced dye degradation and reactive radical generation (Fig. 8a).

Tan *et al.* introduced wrinkled structures of varying degrees into 2D carbon nitride (CN) *via* ultrasonication. They established a positive correlation between wrinkle density, the resulting strain gradient, and the intensity of flexoelectric polarization. As shown in Fig. 8b, 700 W ultrasonication treatment of CN (CN700) with large strain gradients induced exhibits enhanced HER performance with a reduced exciton binding energy (from 52 to 34 meV).[32] This indicates that the flexoelectric field significantly lowers the energy barrier for exciton dissociation into free charge carriers (electrons/holes), which directly enhances the population of charges available for the HER.

Liu *et al.* demonstrated that in centrosymmetric semiconductors (δ-MnO_2 and TiO_2 nanoflowers), strain gradient-induced flexoelectric polarization can also enhance photocatalysis.[103] Under ultrasonic stimulation, the dynamic bending of NSs generates a flexoelectric polarization. This polarization drives the photogenerated electron–hole pairs to move in opposite directions, thereby achieving efficient separation of free carriers and causing the energy band to be completely tilted (Fig. 8c). Consequently, the photocatalytic efficiency is largely improved across a broad spectral range from ultraviolet to visible light.

In brief, the coupling of flexoelectricity with photocatalysis is not a single mechanism but a versatile platform. It can be activated *via* intrinsic material properties, engineered through nano-/micro-structuring, or external dynamical excitation, providing multiple avenues to break through the efficiency limits of conventional photocatalysis.

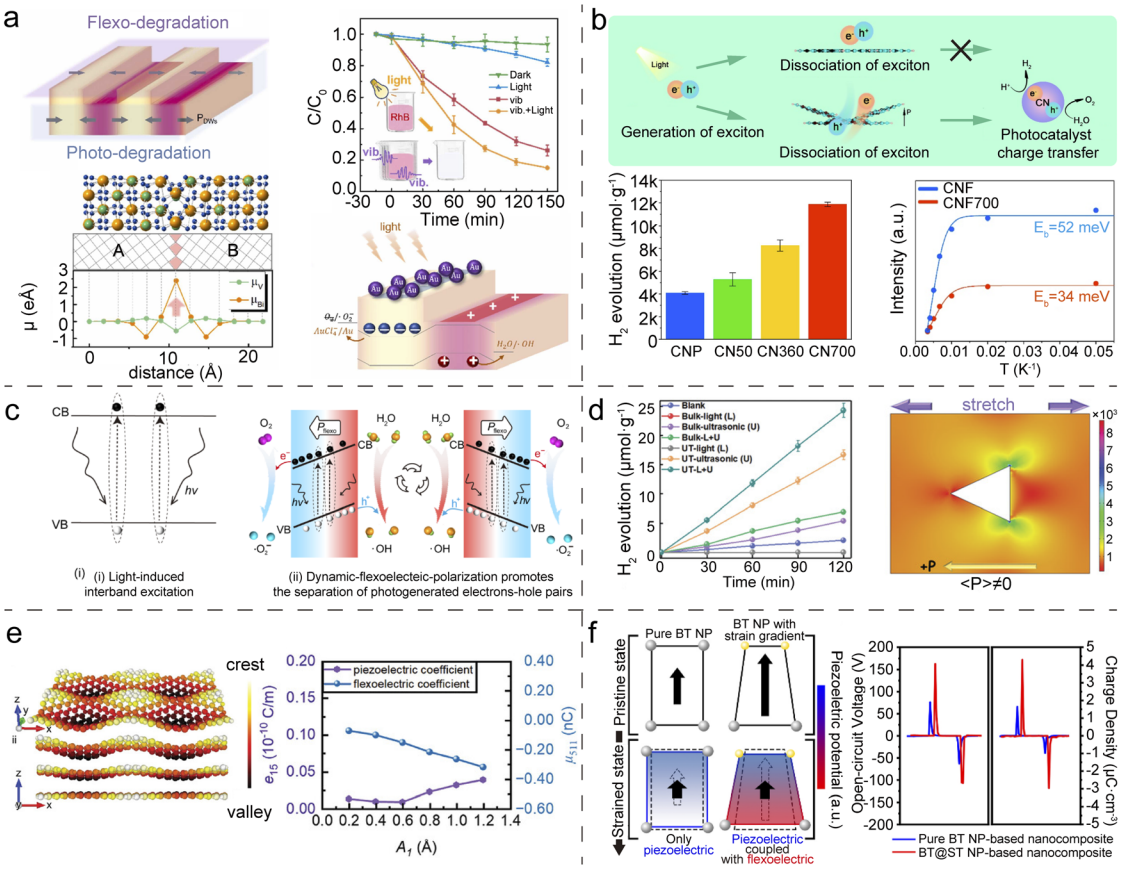

Fig. 8 Hybrid coupling strategies. (a) Schematic illustration of flexo-degradation and photo-degradation processes on BVO; DFT calculations of ferroelastic BVO structures (red arrows represent the net polarization with respect to the center of their surrounding oxygen cages); photo-degradation, flexo-degradation, and flexo–photo-degradation of rhodamine B (RhB) by a BVO film; the flexoelectric potential drives the effective separation of photogenerated carriers, thereby screening surface charges.[102] Copyright 2022 Elsevier. (b) Schematic diagram of exciton transfer in planar and curved CN; H_2 production efficiency *via* flexo–photocatalysis using CN with different curvature degrees; integrated photoluminescence emission intensity as a function of temperature.[32] Copyright 2023 American Chemical Society. (c) Schematic showing the flexo–photocatalysis mechanism of δ-MnO_2 and TiO_2 nanoflowers for organic pollutant degradation; the process of separation and transportation of electrons and holes and the generation of reactive species that participate in the degradation process of organic pollutants under mechanical stimuli.[103] Copyright 2024 Springer Nature Link. (d) H_2 yields and production rates of bulk g-C_3N_4 and UT-g-C_3N_4 under light, ultrasound, and combined light-ultrasound irradiation in pure water; FEM simulation for the stress distribution around a triangular pore in tri-*s*-triazine sheets of g-C_3N_4.[112] Copyright 2021 Wiley-VCH. (e) Spatial diagram of a wrinkled ZnO monolayer; variation patterns of the piezoelectric and flexoelectric coefficient μ_{511} with increasing wrinkle amplitude for the ZnO monolayers.[109] Copyright 2024 Wiley-VCH. (f) Schematic illustrations comparing the piezoelectric potential difference that can be generated inside the lattice of the pure $BaTiO_3$ NP and core–shell NP under pristine and stressed states; output open-circuit voltage signals and charge density measured from nanocomposites made of pure $BaTiO_3$ and $BaTiO_3$@-$SrTiO_3$ NPs under mechanical bending and unbending motions.[113] Copyright 2021 Elsevier.

4.2 Coupling with piezocatalysis

Flexoelectricity can be also coupled with the piezoelectric effect to provide a new approach for mechanical energy harvesting and conversion.[104,105] The core mechanism of this coupling is the simultaneous generation of flexoelectric and piezoelectric polarizations in materials under external mechanical excitations, thus forming superimposed or synergistic internal polarization fields (Fig. 7b).[106,107] This additive effect not only enhances local electric field intensity but also boosts catalytic activity by regulating the energy band structure and carrier distribution, facilitating electron–hole separation and migration to catalytically active sites.[108,109] Furthermore, dynamic excitation causes periodic changes in the polarization fields, driving the directional migration and accumulation of carriers, suppressing electron–hole recombination, prolonging carrier lifetimes, and significantly enhancing catalytic efficiency.[110,111] Meanwhile, this coupling effect also contributes to the adsorption, activation, and dissociation of active intermediates, thus optimizing the catalytic kinetics.[23]

Experimental studies have validated this concept. Hu *et al.* synthesized atomically thin ultrathin graphitic carbon nitride (UT-g-C_3N_4) NSs that show exceptional piezocatalytic H_2 production.[112] They attribute the strong piezoelectric response to in-plane polarization from stacked polar triazine units. Besides, the triangular cavities in g-C_3N_4 NSs may generate strain gradients in the vicinity, which allows a nonzero net average polarization under mechanical vibration owing to the flexoelectric effect. The superposition of piezoelectric and

flexoelectric electric fields forms a combined polarization, which provides a significant electrochemical force to promote water reduction. The UT-g-C_3N_4 NSs achieve an exceptional flexo-piezo-photocatalytic H_2 evolution rate of 12.16 mmol g^{-1} h^{-1} (Fig. 8d).

Yin *et al.* explored the coupling effect of piezo/flexoelectricity, separated the piezoelectric and flexoelectric coefficients, and distinguished the respective contributions to the total polarization by constructing a series of ZnO monolayers with varying wrinkle amplitudes.[109] Piezoelectric and flexoelectric coefficients depend on the wrinkle amplitude. Both coefficients (absolute value) exhibit an escalation with heightened wrinkling, indicating a gradual enhancement in the piezoelectric or flexoelectric effect (Fig. 8e). Polarization $P_x(y)$ results from the synergistic effect of piezoelectric and flexoelectric polarization. Wrinkles in ZnO alter the local electric field, inducing charge and dipole moment changes by piezo/flexoelectric coupling that lead to polarization.

Beyond low-dimensional materials, this coupling strategy also applies to complex nanostructures. Kim *et al.* engineered $BaTiO_3$@$SrTiO_3$ core–shell NPs with a compositional gradient.[113] The lattice mismatch between core and shell creates a substantial strain gradient, which acts to amplify the effective piezoelectric response of the entire NP *via* the flexoelectric effect, leading to enhanced performance (Fig. 8f).

Hence, the coupling of the flexoelectric and piezoelectric effects moves beyond a simple additive model. It establishes a multi-functional materials design paradigm where mechanical energy can be harvested and converted with high efficiency. The growing ability to understand its intrinsic coupling and precisely engineer this coupling in diverse material systems is paving the way for a new generation of high-performance, mechanically driven catalysts.

5. Applications of flexoelectric catalysis

Building on the structural modification strategies and hybrid coupling mechanisms that have significantly enhanced the flexoelectric response and catalytic efficiency of flexoelectric catalysts, they are thus promising in many scenarios. This green, environmentally friendly, and efficient catalytic technology can collect various forms of mechanical energy in nature (*e.g.*, wind and tidal energy) and promote chemical reactions.

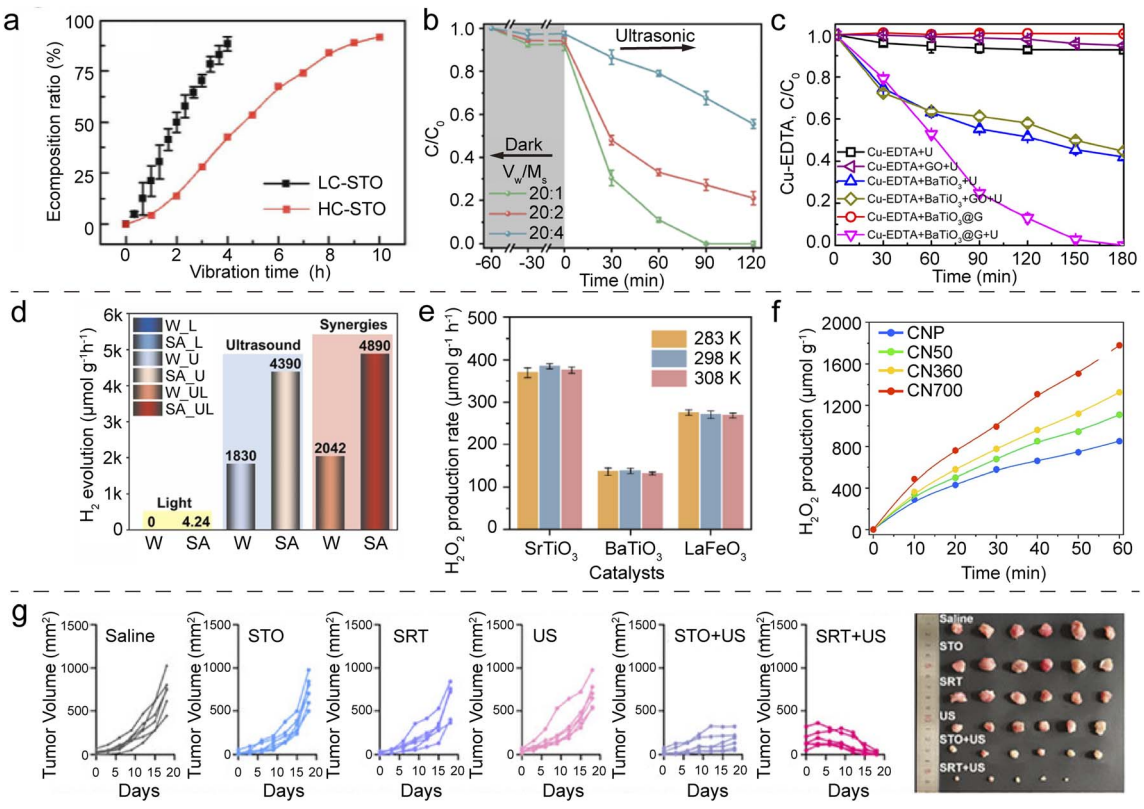

Fig. 9 Applications of flexoelectric catalysis. (a) The extent of discoloration of RhB solutions at evenly spaced intervals by low-crystallinity and high-crystallinity $SrTiO_3$ NPs.[50] Copyright 2022 Wiley-VCH. (b) Degradation under different water–soil ratio conditions (V_w/M_s, mL g^{-1}) by HAP@FAP.[70] Copyright 2023 Royal Society of Chemistry. (c) Comparison of Cu-EDTA removal efficiencies by different catalysts.[116] Copyright 2019 American Chemical Society. (d) H_2 production in pure water (W) and a 0.05 M Na_2SO_3 (SA) sacrificial agent solution under different energy source irradiation conditions.[20] Copyright 2024 Elsevier. (e) H_2O_2 production rates of $SrTiO_3$, $BaTiO_3$, and $LaFeO_3$ NPs at 283 K, 298 K, and 308 K.[28] Copyright 2025 Wiley-VCH. (f) H_2O_2 production efficiency *via* flexo–photocatalysis using CN with different curvature degrees.[32] Copyright 2023 American Chemical Society. (g) Growth curves and photographs of tumors in primary tumors after different treatments.[119] Copyright 2025 Wiley-VCH.

Table 1 Comparison of flexoelectric catalytic performance in degradation of dyes

Catalysts	Detected ROS	Substrate	Reaction rate [min^{-1}]	Catalytic conditions	Ref.
Ag_2MoO_4	$^{\bullet}OH$ and h^+	MB [20 mg L^{-1}]	0.08098	Ultrasound [180 W 40 kHz] 300 W xenon lamp	2021 (ref. 31)
HC-STO	$^{\bullet}OH$ and $^{\bullet}O^{2-}$	RhB [10 mg L^{-1}]	0.008	Ultrasound [240 W 40 kHz]	2022 (ref. 50)
FAP@HAP	$^{\bullet}OH$ and $^{\bullet}O^{2-}$	PHE [200 mg kg^{-1}]	0.01389	Ultrasound [600 W 60 kHz]	2023 (ref. 70)
SA-Pt/CN	$^{\bullet}OH$	RhB [10 mg L^{-1}]	0.00138	Ultrasound [300 W 40 kHz]	2023 (ref. 85)
MnO_2	$^{\bullet}OH$ and $^{\bullet}O^{2-}$	MB/RhB/MO [10 mg^{-1}]	—	Ultrasound [320 W 40 kHz]	2023 (ref. 52)
SnO_2	$^{\bullet}OH$	RhB MB MO [10 mg L^{-1}]	0.008	Ultrasound [500 W]	2024 (ref. 75)
2D TiO_2 NSs	$^{\bullet}OH$ and $^{\bullet}O^{2-}$	RhB [10 mg L^{-1}]	0.015	Ultrasound [—]	2024 (ref. 117)
CeO_2 NRs	h^+ $^{\bullet}OH$ and $^{\bullet}O^{2-}$	RhB [10 mg L^{-1}]	0.065	Ultrasound [180 W 1 MHz]	2024 (ref. 77)
STO-P	$^{\bullet}OH$ and $^{\bullet}O^{2-}$	RhB [5 mg L^{-1}]	0.01905	Ultrasound [200 W 40 kHz]	2025 (ref. 21)
SiO_2	$^{\bullet}OH$ and $^{\bullet}O^{2-}$	RhB [5 mg L^{-1}]	0.05121	Ultrasound [240 W 20 kHz]	2025 (ref. 118)

Consequently, it has received increasing attention and been widely studied in fields such as environmental remediation,[52] energy production,[75] and biomedical therapy.[114]

5.1 Environmental remediation

Flexoelectric catalysis provides a potent mechanical energy-driven approach for eliminating organic pollutants in water, soil, *etc.* The fundamental mechanism involves generating ROS (*i.e.*, reactive oxygen species), such as hydroxyl radicals ($^{\bullet}OH$) and superoxide anions ($^{\bullet}O_2^-$), *via* the flexoelectric polarization field that efficiently separates charge carriers and promotes redox reactions at the surface of catalysts.[75]

A study conducted by Liu *et al.* indicated that the performance of flexoelectric catalysis is pronounced in centrosymmetric $SrTiO_3$ NPs for this application.[50] Due to flexoelectric polarization, $^{\bullet}OH$ and $^{\bullet}O_2^-$ active radicals are periodically generated in the solution, effectively degrading dye molecules such as RhB, methylene blue (MB) and methyl orange (MO) (Fig. 9a). Sheng *et al.* combine flexoelectric catalysis with peroxymonosulfate (PMS) activation, where a flexoelectric field drives electron and hole migration to the reaction interface and activates PMS to degrade organic pollutants rapidly.[115] In soil remediation, the HAP@FAP core–shell structure designed by Han *et al.* achieves a degradation rate of 79% for 200 mg kg^{-1} of phenanthrene (PHE) in soil within 120 minutes (Fig. 9b).[70] Pan *et al.* reported a multifunctional composite NW composed of $BaTiO_3$@graphene that overcomes the challenges associated with Cu and ethylenediaminetetraacetic acid (Cu-EDTA) complex dissociation.[116] The piezoelectric–flexoelectric potential releases Cu(II), and interactions with graphene groups enable Cu recovery (Fig. 9c). Beyond remediation, this work also demonstrates the potential of flexoelectric catalysis in resource recovery from wastewater. Table 1 summarizes the available cases of flexoelectric catalysts for ROS generation and pollutant degradation, highlighting their broad application potential.

5.2 Clean energy production

Flexoelectric catalysis demonstrates considerable potential in the clean energy field, particularly in H_2 and H_2O_2 production.[20,28] Traditional production methods rely on noble metal catalysts and sacrificial agents. In contrast, flexoelectric catalysts, with their wide material space, easy preparation, and flexible conditions, provide an efficient and cost-effective alternative.

Table 2 summarizes the present cases of flexoelectric catalysis for water splitting. For instance, Du *et al.* demonstrated that

Table 2 Comparison of flexoelectric catalytic performance in water splitting

Catalysts	Substrate	Products	Reaction rate [μmol g^{-1} h^{-1}]	Catalytic conditions	Ref.
1T–2H-$MoSe_2$	H_2O	H_2	4858.2	Ultrasound [120–300 W] [20–60 kHz]	2020 (ref. 23)
$Ag(CuZn)(AlCr)_2O_4$/CuO	H_2O	H_2	2116	Ultrasound [300 W 40 kHz]	2023 (ref. 51)
CN700	H_2O	H_2/H_2O_2	11 900	300 W xenon lamp	2023 (ref. 32)
$BiVO_4/Bi_2WO_6$	H_2O	H_2O_2	4860	Ultrasound [300 W 40 kHz] 150 W Xe lamp	2023 (ref. 121)
SA-Pt/CN	H_2O	H_2	1283.8	Ultrasound [300 W 40 kHz]	2023 (ref. 85)
$MAPbI_3$ NWs	HI/H_2O	H_2	756.5	Ultrasound [200 W 100 kHz]	2023 (ref. 24)
2D TiO_2 NSs	H_2O	H_2	137.9	Ultrasound [280 W]	2024 (ref. 117)
CeO_2 NRs	H_2O	H_2	486.4	Ultrasound [180 W 1 MHz]	2024 (ref. 77)
TiO_2	H_2O	H_2	2380	Ultrasound [200 W 40 kHz]	2024 (ref. 20)
$BaTi_2O_5$	H_2O	H_2	1160	Ultrasound [200 W, 40 kHz]	2024 (ref. 26)
$ZnAl_2O_4$	H_2O	H_2	3737.6	Ultrasound [300 W 40 kHz]	2025 (ref. 22)
F-HAP	H_2O	H_2	322.7	Ultrasound [100 W 100 kHz]	2025 (ref. 89)

rutile TiO_2 achieves an H_2 production rate of 2380 μmol g^{-1} h^{-1} under flexoelectric catalysis (Fig. 9d). Mondal *et al.* reported that centrosymmetric $SrTiO_3$ NPs reach a H_2 production rate of 1289.5 μmol g^{-1} h^{-1}.[21] Pan *et al.* proposed enhancing flexoelectric catalytic efficiency by controlling the intrinsic magnetism of the catalyst. The paramagnetic-to-antiferromagnetic transition in $LaCrO_3$ significantly boosts the flexoelectric polarization, increasing H_2O_2 yield by 90% (Fig. 9e).[28] Tan *et al.* reported that CN prepared *via* ultrasonic treatment and combined with light irradiation achieves rapid H_2 evolution at 11.9 mmol g^{-1} h^{-1} and efficient H_2O_2 generation at 1779 μmol g^{-1} (Fig. 9f).[32] These studies further prove the high efficiency of flexoelectric catalysis.

5.3 Biomedical applications

Flexoelectric catalysis demonstrates unique advantages in the field of tumor therapy by disrupting mitochondrial function, alleviating hypoxia, and generating ROS.[114] In biomedicine, flexoelectric catalysis introduces a novel physical mechanism for tumor therapy, primarily by disrupting cellular energy metabolism and modulating the tumor microenvironment.

A seminal study by Fu *et al.* uses $SrTiO_3$/RGD/TPP (SRT) to disrupt the balance between proton gradient and ionic equilibrium in mitochondria using ultrasound-induced flexoelectric catalysis (Fig. 9g).[119] Li *et al.* proposed WS_2/Pt Schottky heterojunctions as a "dual-mode" therapy platform that utilizes flexoelectric catalysis to disrupt the tumor's interstitial fluid pressure (IFP), generating oxygen and active oxygen species while relieving IFP, thereby providing an innovative strategy for comprehensive tumor therapy.[53] Building on this, they developed an advanced biomimetic nanomedicine (MPI@M) based on $MoSe_2$/Pt Schottky junctions combined with a photosensitizer.[120] Under acoustic stimulation, MPI@M decomposes water in the tumor interstitial liquid, reducing IFP and releasing oxygen to overcome hypoxia, thereby enhancing photodynamic therapy efficacy and disrupting mitochondrial function. These research findings highlight the considerable potential of flexoelectric catalysis in improving tumor treatment outcomes and overcoming the limitations of conventional therapies.

In short, flexoelectric catalysis showcases broad application prospects in key areas (environmental remediation, clean energy, biomedicine, *etc.*). Through strain gradient-induced polarization effects, flexoelectric catalysis can efficiently degrade organic pollutants, remove heavy metals, and enhance the efficiency of H_2 and H_2O_2 production. Furthermore, the unique advantages of flexoelectric catalysis in tumor therapy provide new strategies for precision medicine. As research deepens and technology advances, flexoelectric catalysis is expected to provide innovative solutions to global environmental, energy, and health challenges.

We would like to add here that several notable practical challenges remain to be addressed in flexoelectric catalytic experiments. For instance, prolonged dynamic strain/stress may lead to material aging and stress gradient decay. Furthermore, systematic optimization is required to enhance the overall energy utilization efficiency. Besides, there is currently a lack of a universal approach for assessing the actual energy conversion efficiency, due to the complexity of multiple energy interacting mechanisms, combined with inconsistent testing protocols among different research teams. Additionally, there are currently no established cases of large-scale manufacturing or implementation of flexoelectric catalysts. Therefore, advancing this novel catalytic technology requires more profound investigations into its fundamental principles and practical deployment.

6 Summary and perspectives

As shown above, flexoelectric catalysis has emerged as a promising mechanism for promoting diverse reactions by the strain gradient-induced polarization fields that govern essential processes such as band bending, charge separation, and surface activation of catalysts. This capability has been successfully demonstrated in applications ranging from environmental remediation and energy production to biomedical therapy. To harness this potential, scientists have developed strategies centered on amplifying the intrinsic flexoelectric response, chiefly *via* multi-scale strain gradient engineering including geometric structure design, interface engineering, and atomic-scale doping/defect introduction. Concurrently, coupling flexoelectricity with the fundamental processes of other catalysis mechanisms (*e.g.*, photocatalysis and piezocatalysis) has unlocked synergistic effects that further improve the catalytic activity. In the following text, we briefly propose the current technical challenges as well as the future research highlights for this emerging field.

6.1 Technical challenges for flexoelectric catalysis

Flexoelectric catalysis has gained considerable attention because of its potential in enhancing reaction efficiencies and promoting novel chemical transformations. However, its practical implementation still requires overcoming several hurdles, including the accurate theoretical prediction of flexoelectric properties, the precise engineering of strain gradients, and the understanding of coupling effects with other catalytic mechanisms.

6.1.1 Theoretical predictions of flexoelectric properties and catalytic effects of materials. Theoretical modeling of flexoelectricity is inherently difficult for several reasons, including the presence of higher-order partial differential equations, nonlocal effects, and electromechanical couplings within the internal energy. Moreover, the use of various definitions for deformation metrics, along with the requirement for more detailed governing equations and boundary conditions, adds to the difficulty.[122] While DFT[14] is powerful for calculating fundamental properties at the atomic scale and FEM can simulate strain fields at the continuum level,[115,116] seamlessly integrating these across scales to predict flexoelectric properties and even catalytic effects of materials can be exceptionally challenging.[17,123,124] The recent progress in multi-scale modeling that combines continuum mechanics with atomistic simulations may aid in predicting the details of flexoelectric catalysis.

Machine learning for high-throughput catalyst screening and advanced microfluidic/nanofluidic technologies can help to release the practical potential of flexoelectric catalysts.

6.1.2 Precise characterization and engineering of strain gradients. One of the major challenges in flexoelectric catalysis is the precise characterization and engineering of strain gradients in catalysts. At present, high-resolution transmission electron microscopy images together with GPA analysis enable the visualization of lattice distortions, while X-ray diffraction and X-ray absorption fine structure spectra provide indirect evidence of lattice strain *via* revealing the microscopic characteristics of lattice spacing and local coordination environments. However, as flexoelectric catalysis is a highly dynamic process in multi-phased environments, these conventional characterization techniques are insufficient to capture its dynamic nature.

6.1.3 Understanding the synergistic effect of flexoelectric catalysis with other catalytic mechanisms. As an emerging subfield of mechanocatalysis, flexoelectric catalysis has achieved remarkable progress in both fundamental understanding and practical applications. However, the in-depth understanding of its microscopic process and coupling mechanism with other catalytic technologies remains obscure. Considering its ubiquity in materials, flexoelectricity can be coupled with photocatalysis, piezocatalysis, pyrocatalysis, *etc.* to boost the overall performance; the coupling involves complex physicochemical processes such as charge transfer, energy exchange, and active site modulation, rendering it challenging to disentangle their contributions.

6.2 Future prospects

In view of the above technical challenges, the future study of flexoelectric catalysis is full of opportunities. Building on the current understanding and technological advancements, several possible directions are proposed for advancing this emerging field.

6.2.1 Design of novel catalysts. Given the urgent demand for superior catalytic performance and broad application scenarios, the search for novel flexoelectric catalysts is definitely a key direction, just as what happened in other catalytic cases. In this regard, traditional trial-and-error approaches are inefficient and time-consuming. Modern computational techniques, such as high-throughput screening and machine learning-driven performance prediction, provide a powerful tool for discovering high-performance catalysts. These methods can effectively screen potential candidate materials from large material libraries, guiding experimental efforts toward the most promising directions.

6.2.2 Implementation of *in situ*/*operando* characterization. *In situ*/*operando* characterization techniques are essential for understanding the dynamic behavior of flexoelectric catalysis. Future research should consider using advanced *in situ*/*operando* characterization methods, including transmission electron microscopy, surface-enhanced Raman spectroscopy, shell-isolated NP-enhanced Raman spectroscopy, and X-ray absorption spectroscopy. These techniques can quantify the effects of various distortion sources (such as doping, defects, and heterojunctions) on electronic states and active site structures of catalysts, as well as monitor the dynamic evolution of strain gradients, polarization fields, and surface reaction intermediates during catalysis. These technologies are also expected to identify active sites and reaction intermediates during catalysis, providing valuable information for catalyst design and optimization.

6.2.3 Expansion of new application scenarios. By reducing energy barriers and enabling flexible, low-cost catalysts, flexoelectric catalysis holds transformative potential for clean energy technologies and carbon neutrality goals. It enhances the efficiency of the HER/OER and promotes advancements toward global sustainability. However, beyond current applications (environmental remediation, renewable energy, and biomedicine), flexoelectric catalysis could revolutionize industries by being applied to emerging scenarios such as nitrogen fixation, carbon dioxide reduction, and selective organic synthesis, and its application scope can be further expanded *via* multi-field coupling approaches to realize an industrial revolution. Thus, flexoelectric catalysis is anticipated to bridge fundamental materials science with scalable clean energy solutions, which are pivotal in advancing next-generation sustainable technologies.

Author contributions

All authors conceived idea for the project and wrote the manuscript.

Conflicts of interest

There are no conflicts to declare.

Data availability

No primary research results, software or code have been included and no new data were generated or analyzed as part of this review.

Acknowledgements

This work was supported by the National Natural Science Foundation of China (52562035, 22375081 and U21A20500). L. F. also acknowledges the support from Nanchang University.

References

1 J.-W. Zhao, H.-Y. Wang, L. Feng, J.-Z. Zhu, J.-X. Liu and W.-X. Li, Crystal-phase engineering in heterogeneous catalysis, *Chem. Rev.*, 2024, **124**, 164.
2 J. Li, R. Güttinger, R. Moré, F. Song, W. Wan and G. R. Patzke, Frontiers of water oxidation: The quest for true catalysts, *Chem. Soc. Rev.*, 2017, **46**, 6124.
3 A. I. Osman, A. M. Elgarahy, A. S. Eltaweil, E. M. Abd El-Monaem, H. G. El-Aqapa, Y. Park, Y. Hwang, A. Ayati, M. Farghali, I. Ihara, A. a. H. Al-Muhtaseb, D. W. Rooney, P.-S. Yap and M. Sillanpää, Biofuel production, hydrogen

production and water remediation by photocatalysis, biocatalysis and electrocatalysis, *Environ. Chem. Lett.*, 2023, **21**, 1315.
4 P. Jia, J. Li and H. Huang, Piezocatalysts and piezo-photocatalysts: From material design to diverse applications, *Adv. Funct. Mater.*, 2024, **34**, 2407309.
5 Q. Pei, Y. Wang, K. C. Tan, J. Guo, T. He and P. Chen, Hydrogen production via photocatalytic ammonia decomposition, *Chem. Sci.*, 2025, **16**, 9076.
6 S. Li, J. Liu, Z. L. Wang and D. Wei, Mechano-driven chemical reactions, *Green Energy Environ.*, 2025, **10**, 937.
7 S. Wang, X. Wang, W. Tong, X. Li and Y. Zhang, Microstructure designed flexoelectric materials and tip force for multifunctional applications, *Nano Energy*, 2025, **133**, 110442.
8 J. Liu, W. Qi, M. Xu, T. Thomas, S. Liu and M. Yang, Piezocatalytic techniques in environmental remediation, *Angew. Chem., Int. Ed.*, 2023, **62**, e202213927.
9 T. D. Nguyen, S. Mao, Y.-W. Yeh, P. K. Purohit and M. C. McAlpine, Nanoscale flexoelectricity, *Adv. Mater.*, 2013, **25**, 946.
10 X. Wang, J. M. Wu and L. Li, Fundamentals and applications of piezotronics for catalysis, *MRS Bull.*, 2025, **50**, 165.
11 N. Meng, W. Liu, R. Jiang, Y. Zhang, S. Dunn, J. Wu and H. Yan, Fundamentals, advances and perspectives of piezocatalysis: A marriage of solid-state physics and catalytic chemistry, *Prog. Mater. Sci.*, 2023, **138**, 101161.
12 X. Jia, R. Guo, J. Chen and X. Yan, Flexoelectric effect in thin films: Theory and applications, *Adv. Funct. Mater.*, 2025, **35**, 2412887.
13 X. Jiang, W. Huang and S. Zhang, Flexoelectric nano-generator: Materials, structures and devices, *Nano Energy*, 2013, **2**, 1079.
14 M. Mohammadkhah, V. Slavkovic and S. Klinge, Flexoelectricity in biological materials and its potential applications in biomedical research, *Bioengineering*, 2025, **12**, 579.
15 B. Wang, Y. Gu, S. Zhang and L.-Q. Chen, Flexoelectricity in solids: Progress, challenges, and perspectives, *Prog. Mater. Sci.*, 2019, **106**, 100570.
16 L. Shu, R. Liang, Z. Rao, L. Fei, S. Ke and Y. Wang, Flexoelectric materials and their related applications: A focused review, *J. Adv. Ceram.*, 2019, **8**, 153.
17 E. A. k. Ali and N. M. Faleh, Flexoelectric effects of nanoscale electrical materials under dynamic conditions, *Energy Sci. Eng.*, 2025, **13**, 4348.
18 S. Das, B. Wang, T. R. Paudel, S. M. Park, E. Y. Tsymbal, L.-Q. Chen, D. Lee and T. W. Noh, Enhanced flexoelectricity at reduced dimensions revealed by mechanically tunable quantum tunnelling, *Nat. Commun.*, 2019, **10**, 537.
19 M. Kołodziej, N. Ojha, M. Budziałowski, K. Załęski, I. Fina, Y. K. Mishra, K. K. Pant and E. Coy, Fundamentals of flexoelectricity, materials and emerging opportunities toward strain-driven nanocatalysts, *Small*, 2024, **20**, 2406726.
20 Y. Du, S. Zhang and Z. Cheng, Flexocatalysis of nanoscale titanium dioxide, *Nano Energy*, 2024, **127**, 109731.
21 S. Mondal, R. C. Das, Y. Du, Z. Hou, K. Konstantinov and Z. Cheng, Flexocatalytic hydrogen generation and organics degradation by nano $SrTiO_3$, *Adv. Sci.*, 2025, **12**, 2500034.
22 K. Y. Tu, H.-Y. Lin, J.-P. Chou and J. M. Wu, Unveiling the flexocatalytic potential of wide-bandgap spinel oxides: Light-free hydrogen evolution via strain-induced polarization and oxygen vacancy engineering, *Adv. Funct. Mater.*, 2025, **35**, 2424279.
23 Y.-J. Chung, C.-S. Yang, J.-T. Lee, G. H. Wu and J. M. Wu, Coupling effect of piezo–flexocatalytic hydrogen evolution with hybrid 1T- and 2H-phase few-layered $MoSe_2$ nanosheets, *Adv. Energy Mater.*, 2020, **10**, 2002082.
24 Y. Zhang, J. Huang, M. Zhu, Z. Zhang, K. Nie, Z. Wang, X. Liao, L. Shu, T. Tian, Z. Wang, Y. Lu and L. Fei, Significant hydrogen generation via photo-mechanical coupling in flexible methylammonium lead iodide nanowires, *Chem. Sci.*, 2024, **15**, 1782.
25 Y. Jiang, J. Liang, F. Zhuo, H. Ma, S. S. Mofarah, C. C. Sorrell, D. Wang and P. Koshy, Unveiling mechanically driven catalytic processes: Beyond piezocatalysis to synergetic effects, *ACS Nano*, 2025, **19**, 18037.
26 Y. Du, W. Sun, X. Li, C. Hao, J. Wang, Y. Fan, J. Joseph, C. Yang, Q. Gu, Y. Liu, S. Zhang and Z. Cheng, Mechanocatalytic hydrogen generation in centrosymmetric barium dititanate, *Adv. Sci.*, 2024, **11**, 2404483.
27 J. Xu, X. Zhang, X. Liu, M. Wu, J. Liu, Z. Liu, M. Li, Y. Yue, Y. Xu, C. Dong, W. Zheng, L. Zhu, Y. Cao, C. Zheng, J. Liu, A. Li, D. Wu, L. Zhang and Z. Wen, Enhanced oxygen evolution reaction in flexoelectric thin-film heterostructures, *Appl. Phys. Rev.*, 2024, **11**, 041419.
28 Y. Pan, R. Li, L. Zhang, J.-X. Liu, W. Wang and G.-J. Zhang, Enhancing flexoelectric catalytic performance by modulating the intrinsic magnetism of $LaCrO_3$, *Adv. Funct. Mater.*, 2026, **36**, e12272.
29 Y. Bian, W. Liu, Y. Fan, Y. Qi, C. Liu, S. Zhao, Y. Wang, D. Luo, Y. Zhou, Y. Liu and J. Song, Flexoelectric polarization unlocks hidden catalytic power in MnO_2 nanoflowers: ROS-mediated pathogen elimination and infected wound regeneration, *Nano Res.*, 2025, **18**, 94907664.
30 L. Su, J. Xu, R. Huang, J. Liao, L. Zhao, L. Li, Z. Zhang and Y. Xiong, Flexoelectric polarization-enhanced Gd-based nanoflowers for efficient phosphatase-mimicking dephosphorylation, *Small Struct.*, 2025, DOI: 10.1002/sstr.202500559.
31 T. Cheng, H. Gao, R. Li, S. Wang, Z. Yi and H. Yang, Flexoelectricity-induced enhancement in carrier separation and photocatalytic activity of a photocatalyst, *Appl. Surf. Sci.*, 2021, **566**, 150669.
32 H. Tan, W. Si, W. Peng, X. Chen, X. Liu, Y. You, L. Wang, F. Hou and J. Liang, Flexo-/piezoelectric polarization

boosting exciton dissociation in curved two-dimensional carbon nitride photocatalyst, *Nano Lett.*, 2023, **23**, 10571.
33 P. Jia, Y. Yu, T. Chen and H. Huang, "Electricity"-assisted catalytic solar-to-fuel processes, *Angew. Chem., Int. Ed.*, 2025, **64**, e202508809.
34 S. Krichen and P. Sharma, Flexoelectricity: A perspective on an unusual electromechanical coupling, *J. Appl. Mech.*, 2016, **83**, 030801.
35 D. Tian, D.-Y. Jeong, Z. Fu and B. Chu, Flexoelectric effect of ferroelectric materials and its applications, *Actuators*, 2023, **12**, 114.
36 V. Mashkevich and K. Tolpygo, Electrical, optical and elastic properties of diamond type crystals, *Sov. Phys. JETP*, 1957, **5**, 435.
37 S. M. Kogan, Piezoelectric effect during inhomogeneous deformation and acoustic scattering of carriers in crystals, *Sov. Phys. Solid State*, 1964, **5**, 2067.
38 R. D. Mindlin, Polarization gradient in elastic dielectrics, *Int. J. Solids Struct.*, 1968, **4**, 637.
39 A. Askar and P. C. Y. Lee, Lattice-dynamics approach to the theory of diatomic elastic dielectrics, *Phys. Rev. B*, 1974, **9**, 5291.
40 V. Indenbom, E. Loginov and M. Osipov, The flexoelectric effect and the structure of crystals, *Sov. Phys. Crystallogr.*, 1981, **26**, 656.
41 V. Indenbom, E. Loginov and M. Osipov, Flexoelectric effect and structure of crystals, *Kristallografiya*, 1981, **28**, 1157.
42 A. K. Tagantsev, Electric polarization in crystals and its response to thermal and elastic perturbations, *Phase Transitions*, 1991, **35**, 119.
43 W. Ma and L. E. Cross, Strain-gradient-induced electric polarization in lead zirconate titanate ceramics, *Appl. Phys. Lett.*, 2003, **82**, 3293.
44 J. Y. Fu, W. Zhu, N. Li and L. E. Cross, Experimental studies of the converse flexoelectric effect induced by inhomogeneous electric field in a barium strontium titanate composition, *J. Appl. Phys.*, 2006, **100**, 024112.
45 M. S. Majdoub, P. Sharma and T. Cagin, Enhanced size-dependent piezoelectricity and elasticity in nanostructures due to the flexoelectric effect, *Phys. Rev. B: Condens. Matter Mater. Phys.*, 2008, **77**, 125424.
46 J. Narvaez, F. Vasquez-Sancho and G. Catalan, Enhanced flexoelectric-like response in oxide semiconductors, *Nature*, 2016, **538**, 219.
47 L. Shu, S. Ke, L. Fei, W. Huang, Z. Wang, J. Gong, X. Jiang, L. Wang, F. Li, S. Lei, Z. Rao, Y. Zhou, R.-K. Zheng, X. Yao, Y. Wang, M. Stengel and G. Catalan, Photoflexoelectric effect in halide perovskites, *Nat. Mater.*, 2020, **19**, 605.
48 M.-M. Yang, D. J. Kim and M. Alexe, Flexo-photovoltaic effect, *Science*, 2018, **360**, 904.
49 L. Wang, S. Liu, X. Feng, C. Zhang, L. Zhu, J. Zhai, Y. Qin and Z. L. Wang, Flexoelectronics of centrosymmetric semiconductors, *Nat. Nanotechnol.*, 2020, **15**, 661.
50 Z. Liu, X. Wen, Y. Wang, Y. Jia, F. Wang, G. Yuan and Y. Wang, Robust flexo-catalysis in centrosymmetric nanoparticles, *Adv. Mater. Technol.*, 2022, **7**, 2101484.
51 P. Y. Wu, K. T. Le, H. Y. Lin, Y. C. Chen, P. H. Wu and J. M. Wu, Flexoelectric catalysts based on hierarchical wrinkling surface of centrosymmetric high-entropy oxide, *ACS Nano*, 2023, **17**, 17417.
52 T. Wu, K. Liu, S. Liu, X. Feng, X. Wang, L. Wang, Y. Qin and Z. L. Wang, Highly efficient flexocatalysis of two-dimensional semiconductors, *Adv. Mater.*, 2023, **35**, 2208121.
53 A. Li, T. Zhang, X. Zhang, Z. Xu, H. Liu, M. Yuan, X. Wei, Y. Zhu, W. Tu, X. Jiang and Y. He, Flexocatalytic reduction of tumor interstitial fluid/solid pressure for efficient nanodrug penetration, *ACS Nano*, 2024, **18**, 5344.
54 B. Li, S. Wang, C. Liu, Y. Xu, W. Deng, J. Yuan, J. Zhao, W. Yang and X. Li, Bending induced polarization charges in non-polar porous polymer for stroke rehabilitation, *Chem. Eng. J.*, 2024, **493**, 152684.
55 B. Wang, Y. Gu, S. Zhang and L. Q. Chen, Flexoelectricity in solids: Progress, challenges, and perspectives, *Prog. Mater. Sci.*, 2019, **106**, 100570.
56 P. Zubko, G. Catalan and A. K. Tagantsev, Flexoelectric effect in solids, *Annu. Rev. Mater. Res.*, 2013, **43**, 387.
57 K. Liu, S. Shao, H. Ji, T. Wu, S. Shen, S. Zhang and M. Xu, Enhanced flexoelectricity with pre-strain gradients, *Appl. Phys. Lett.*, 2022, **121**, 042904.
58 S. Chandrasekaran, Q. Wang, Q. Liu, H. Wang, D. Qiu, H. Lu, Y. Liu, C. Bowen and H. Huang, Dynamic regulation of ferroelectric polarization using external stimuli for efficient water splitting and beyond, *Chem. Soc. Rev.*, 2025, **54**, 2275.
59 C. Guan, X. Yue and Q. Xiang, The role of lattice distortion in catalysis: Functionality and distinctions from strain, *Adv. Mater.*, 2025, **37**, 2501209.
60 X. Yang, Y. Wang, X. Tong and N. Yang, Strain engineering in electrocatalysts: Fundamentals, progress, and perspectives, *Adv. Energy Mater.*, 2022, **12**, 2102261.
61 X. Liang, H. Dong, Y. Wang, Q. Ma, H. Shang, S. Hu and S. Shen, Advancements of flexoelectric materials and their implementations in flexoelectric devices, *Adv. Funct. Mater.*, 2024, **34**, 2409906.
62 C. Wei, J. Tang and W. Huang, Size-dependent effect of the flexoelectronics in a composite beam, *Acta Mech.*, 2024, **235**, 925.
63 D. Lee, A. Yoon, S. Y. Jang, J. G. Yoon, J. S. Chung, M. Kim, J. F. Scott and T. W. Noh, Giant flexoelectric effect in ferroelectric epitaxial thin films, *Phys. Rev. Lett.*, 2011, **107**, 057602.
64 S. Mao and P. K. Purohit, Defects in flexoelectric solids, *J. Mech. Phys. Solids*, 2015, **84**, 95.
65 Z. Wang, C. Li, H. Xie, Z. Zhang, W. Huang, S. Ke and L. Shu, Effect of grain size on flexoelectricity, *Phys. Rev. Appl.*, 2022, **18**, 064017.
66 X. Yang, B. Xia, X. Guo, Y. Qi, Z. Wang, Z. Fu, Y. Chen, R. Zuo and B. Chu, Grain size effect of the flexoelectric response in $BaTiO_3$ ceramics, *J. Appl. Phys.*, 2024, **135**, 024103.

67 B. T. Sneed, A. P. Young and C.-K. Tsung, Building up strain in colloidal metal nanoparticle catalysts, *Nanoscale*, 2015, **7**, 12248.
68 T. Wu, M. Sun and B. Huang, Atomic-strain mapping of high-index facets in late-transition-metal nanoparticles for electrocatalysis, *Angew. Chem., Int. Ed.*, 2021, **60**, 22996.
69 K. R. Beyerlein, R. L. Snyder, M. Li and P. Scardi, Simulation and modeling of nanoparticle surface strain, *J. Nanosci. Nanotechnol.*, 2012, **12**, 8554.
70 J. Han, W. Tian, Y. Miao, N. Li, D. Chen, Q. Xu, H. Li and J. Lu, Flexoelectricity in hydroxyapatite for the enhanced piezocatalytic degradation of phenanthrene in soil, *Ind. Chem. Mater.*, 2024, **2**, 300.
71 M. Zhang, D. Yan, J. Wang and L.-H. Shao, Ultrahigh flexoelectric effect of 3D interconnected porous polymers: Modelling and verification, *J. Mech. Phys. Solids*, 2021, **151**, 104396.
72 S. Zhang, K. Liu, T. Wu, M. Xu and S. Shen, An electro-mechanical behavior enhancement method: Geometric design with flexoelectricity, *Smart Mater. Struct.*, 2019, **28**, 025024.
73 L. Zhu, R. Liang, Z. Wang, M. Ye, J. Gu, Z. Liu, R. Zheng, S. Ke and L. Shu, One-dimensional wrinkled $SrRuO_3$ single-crystalline thin films with tunable strain gradients, *Phys. Rev. Mater.*, 2025, **9**, 014401.
74 Y. Li, Q. Zhou, J. Wu, J. Xu, W. Shi, C. Su, D. Chen and Z. Shao, Controllably grown single-crystal films as flexoelectric nanogenerators for continuous direct current output, *npj Flexible Electron.*, 2022, **6**, 88.
75 N.-J. Chang, Y.-C. Chen, S.-N. Lai and J. Ming Wu, Enhancing dye degradation in darkness: The role of SnO_2 nanorod clusters in flexocatalysis, *Chem. Eng. J.*, 2024, **494**, 152795.
76 J. Mahajan, S. Dhingra, A. Babu, A. P. Singh Rana, A. Jaryal, C. Bera, D. Mandal and K. Kailasam, Flexocatalytically driven water splitting: Unprecedented hydrogen production using symmetry invariant $ZnIn_2S_4$ nanosheets, *J. Mater. Chem. A*, 2025, **13**, 37962.
77 L. Sai, Y. Xiao, F. Yan, T. Ying, Z. Wu, H. Xu, Y. Jia and F. Wang, Integration of hydrogen evolution and dye removal in flexocatalysis by centrosymmetric semiconductor nanorods, *Int. J. Hydrogen Energy*, 2024, **69**, 944.
78 R. P. Jansonius, L. M. Reid, C. N. Virca and C. P. Berlinguette, Strain engineering electrocatalysts for selective CO_2 reduction, *ACS Energy Lett.*, 2019, **4**, 980.
79 Y. Liao, R. He, W. Pan, Y. Li, Y. Wang, J. Li and Y. Li, Lattice distortion induced Ce-doped NiFe-LDH for efficient oxygen evolution, *Chem. Eng. J.*, 2023, **464**, 142669.
80 Y. Xiong, Z. Luo, W. Chen, Z. Li, S. Yin, C. Peng, J. Hong, J. Qi, M.-Q. Cai, Z. Xiao, C. Ma and S. Chen, Atomic-scale insights into flexoelectricity and the enhanced photovoltaic effect at the grain boundary in halide perovskites, *Nano Lett.*, 2025, **25**, 9734.
81 H. Song, S.-Y. Hwang, K.-D. Sung, X. Cheng, J. H. Jung, J.-M. Park, A. Kumar, K. H. Kim, S.-Y. Chung, S.-W. Kim, L.-Q. Chen, C.-B. Eom, D.-Y. Jeong, S.-Y. Choi and J. Ryu, Localized flexoelectric effect around Ba(CuNb) nano-clusters in epitaxial $BiFeO_3$ films for enhancement of electric and multiferroic properties, *Adv. Funct. Mater.*, 2025, **35**, 2416179.
82 E. A. Eliseev, A. N. Morozovska, Y. Gu, A. Y. Borisevich, L.-Q. Chen, V. Gopalan and S. V. Kalinin, Conductivity of twin-domain-wall/surface junctions in ferroelastics: Interplay of deformation potential, octahedral rotations, improper ferroelectricity, and flexoelectric coupling, *Phys. Rev. B: Condens. Matter Mater. Phys.*, 2012, **86**, 085416.
83 Y. T. Wang, H. Y. Lin, Y. C. Chen, Y. G. Lin and J. M. Wu, Piezo-flexocatalysis of single-atom Pt-loaded graphitic carbon nitride, *Small Methods*, 2023, **8**, 2301287.
84 M. Pu, D. Wang, Z. Zhang, Y. Guo and W. Guo, Flexoelectricity enhanced water splitting and hydrogen evolution reaction on grain boundaries of monolayer transition metal dichalcogenides, *Nano Res.*, 2022, **15**, 978.
85 Y. T. Wang, H.-Y. Lin, Y.-C. Chen, Y.-G. Lin and J. M. Wu, Piezo-flexocatalysis of single-atom Pt-loaded graphitic carbon nitride, *Small Methods*, 2024, **8**, 2301287.
86 R. Su, Z. Wang, L. Zhu, Y. Pan, D. Zhang, H. Wen, Z.-D. Luo, L. Li, F.-t. Li, M. Wu, L. He, P. Sharma and J. Seidel, Strain-engineered nano-ferroelectrics for high-efficiency piezocatalytic overall water splitting, *Angew. Chem., Int. Ed.*, 2021, **60**, 16019.
87 G. Wu, X. Han, J. Cai, P. Yin, P. Cui, X. Zheng, H. Li, C. Chen, G. Wang and X. Hong, In-plane strain engineering in ultrathin noble metal nanosheets boosts the intrinsic electrocatalytic hydrogen evolution activity, *Nat. Commun.*, 2022, **13**, 4200.
88 L. Zhang, Z. Wang, S. Shu, Y. Hu, C. Li, S. Ke, F. Li and L. Shu, Origin of defects induced large flexoelectricity in ferroelectric ceramics, *Phys. Rev. Mater.*, 2022, **6**, 094416.
89 Y. Zhang, J. Huang, L. Jiang, J. Qiang, Z. Zhang, Z. Liu, Y. Liu, T. Tian, Z. Wang and L. Fei, Boosting hydrogen evolution via flexoelectric catalysis in gradient F-doped hydroxyapatite nanowires, *Chem. Sci.*, 2025, **16**, 9905.
90 H. Che, X. Wang, H. Yue, C. Chen, D. Xie, S. Yang, B. Liu and Y. Ao, Precise regulation of d-band centers inducing to high-efficiency dual-channel piezocatalytic H_2O_2 production, *Adv. Funct. Mater.*, 2026, **36**, e16979.
91 H. Shi, Y. Liu, Y. Bai, H. Lv, W. Zhou, Y. Liu and D.-G. Yu, Progress in defect engineering strategies to enhance piezoelectric catalysis for efficient water treatment and energy regeneration, *Sep. Purif. Technol.*, 2024, **330**, 125247.
92 Q. Ma, X. Wen, L. Lv, Q. Deng and S. Shen, On the flexoelectric-like effect of Nb-doped $SrTiO_3$ single crystals, *Appl. Phys. Lett.*, 2023, **123**, 082902.
93 Y.-C. Chen, P.-H. Chen, Y.-S. Liao, J.-P. Chou and J. M. Wu, Defect engineering centrosymmetric 2D material flexocatalysts, *Small*, 2024, **20**, 2401116.
94 M. Pu, Y. Guo and W. Guo, Wrinkle facilitated hydrogen evolution reaction of vacancy-defected transition metal dichalcogenide monolayers, *Nanoscale*, 2021, **13**, 20576.
95 D. Mateo, J. L. Cerrillo, S. Durini and J. Gascon, Fundamentals and applications of photo-thermal catalysis, *Chem. Soc. Rev.*, 2021, **50**, 2173.

96 M. Wang, Y. Zuo, J. Wang, Y. Wang, X. Shen, B. Qiu, L. Cai, F. Zhou, S. P. Lau and Y. Chai, Remarkably enhanced hydrogen generation of organolead halide perovskites via piezocatalysis and photocatalysis, *Adv. Energy Mater.*, 2019, **9**, 1901801.

97 Y. Miao, Y. Zhao, S. Zhang, R. Shi and T. Zhang, Strain engineering: A boosting strategy for photocatalysis, *Adv. Mater.*, 2022, **34**, 2200868.

98 A. K. Moharana and R. Vaish, Flexoelectricity enhanced photocatalysis in $Bi_4Ti_3O_{12}$ for binary dye degradation, *J. Appl. Phys.*, 2025, **138**, 135002.

99 Y. Hu, Y. Pan, Z. Wang, T. Lin, Y. Gao, B. Luo, H. Hu, F. Fan, G. Liu and L. Wang, Lattice distortion induced internal electric field in TiO_2 photoelectrode for efficient charge separation and transfer, *Nat. Commun.*, 2020, **11**, 2129.

100 R. Guo, L. You, W. Lin, A. Abdelsamie, X. Shu, G. Zhou, S. Chen, L. Liu, X. Yan, J. Wang and J. Chen, Continuously controllable photoconductance in freestanding $BiFeO_3$ by the macroscopic flexoelectric effect, *Nat. Commun.*, 2020, **11**, 2571.

101 J. W. Martin, R. I. Slavchov, E. K. Y. Yapp, J. Akroyd, S. Mosbach and M. Kraft, The polarization of polycyclic aromatic hydrocarbons curved by pentagon incorporation: The role of the flexoelectric dipole, *J. Phys. Chem. C*, 2017, **121**, 27154.

102 P.-W. Shao, M.-C. Lin, Q. Zhuang, J. Huang, S. Liu, H.-W. Chen, H.-L. Liu, Y.-J. Lu, Y.-J. Hsu, J.-M. Wu, Y.-C. Chen and Y.-H. Chu, Flexo-phototronic effect in centro-symmetric $BiVO_4$ epitaxial films, *Appl. Catal., B*, 2022, **312**, 121367.

103 K. Liu, T. Wu, L. Xu, Z. Zhang, Z. Liu, L. Wang and Z. L. Wang, Flexo-photocatalysis in centrosymmetric semiconductors, *Nano Res.*, 2024, **17**, 1173.

104 C. Liu, H. Wu and J. Wang, Giant piezoelectric response in piezoelectric/dielectric superlattices due to flexoelectric effect, *Appl. Phys. Lett.*, 2016, **109**, 192901.

105 L. Wang, M. A. Boda, C. Chen, X. He and Z. Yi, Ferroelectric, flexoelectric and photothermal coupling in PVDF-based composites for flexible photoelectric sensors, *Mater. Horiz.*, 2024, **11**, 5295.

106 A. Gaur, C. Porwal, D. Singh, V. S. Chauhan and R. Vaish, Facilitating flexoelectric effect in $BaTiO_3$ ceramic for pollutant removal application via piezocatalysis process, *Colloids Surf., A*, 2024, **689**, 133563.

107 C. Porwal, M. Sharma, A. Gaur, V. S. Chauhan, R. Vaish, I. Kebaili and I. Boukhris, Effect of surface/bulk polarization on piezocatalysis using $BaTiO_3$, *J. Mater. Sci.: Mater. Electron.*, 2024, **35**, 573.

108 X. Zhou, J. Liu, S. Ali, B. Shen, J. Zhai, N. Hedin and J. Yuan, Efficient catalytic production of reactive oxygen species through piezoelectricity in bismuth sulfide rich in sulfur vacancies, *Nano Lett.*, 2024, **24**, 13153.

109 P. Yin, D. Jia, J. Lv, P. Du, M. Willatzen, R. Yang and D. Tan, Coupling of piezo/flexoelectricity and its effect on the band structure of wrinkled ZnO monolayers, *Adv. Funct. Mater.*, 2024, **34**, 2408769.

110 J. Ma, X. Xiong, D. Wu, Y. Wang, C. Ban, Y. Feng, J. Meng, X. Gao, J.-Y. Dai, G. Han, L.-Y. Gan and X. Zhou, Band position-independent piezo-electrocatalysis for ultrahigh CO_2 conversion, *Adv. Mater.*, 2023, **35**, 2300027.

111 C. Yang, L. Zhou, C. Wang, W. Duan, L. Zhang, F. Zhang, J. Zhang, Y. Zhen, L. Gao, F. Fu and Y. Liang, Large-scale synthetic Mo@(2H-1T)-$MoSe_2$ monolithic electrode for efficient hydrogen evolution in all pH scale ranges and seawater, *Appl. Catal., B*, 2022, **304**, 120993.

112 C. Hu, F. Chen, Y. Wang, N. Tian, T. Ma, Y. Zhang and H. Huang, Exceptional cocatalyst-free photo-enhanced piezocatalytic hydrogen evolution of carbon nitride nanosheets from strong in-plane polarization, *Adv. Mater.*, 2021, **33**, 2101751.

113 Y.-g. Kim, H. Kim, G.-J. Lee, H.-U. Lee, S. G. Lee, C. Baek, M.-K. Lee, J.-J. Park, Q. Wang, S. B. Cho, C. K. Jeong and K.-I. Park, Flexoelectric-boosted piezoelectricity of $BaTiO_3$@$SrTiO_3$ core-shell nanostructure determined by multiscale simulations for flexible energy harvesters, *Nano Energy*, 2021, **89**, 106469.

114 O. Ates Sonmezoglu, A. Kamo and S. Sonmezoglu, Phase-oriented zinc stannate nanoparticles via low-temperature green synthesis and their efficacy in piezo/flexo-phototronic antibacterial therapies, *Small*, 2025, **21**, e06793.

115 T. Sheng, H. Cao, W. Liu, S. Lv, X. Liang and S. Shen, Flexocatalysis: Regulating peroxymonosulfate activation by flexoelectricity, *J. Chem. Phys.*, 2025, **162**, 134201.

116 M. Pan, C. Zhang, J. Wang, J. W. Chew, G. Gao and B. Pan, Multifunctional piezoelectric heterostructure of $BaTiO_3$@graphene: Decomplexation of Cu-edta and recovery of Cu, *Environ. Sci. Technol.*, 2019, **53**, 8342.

117 Y. C. Chen, P. H. Chen, Y. S. Liao, J. P. Chou and J. M. Wu, Defect engineering centrosymmetric 2D material flexocatalysts, *Small*, 2024, **20**, 2401116.

118 Y. Zhang, Z. Wu, L. Zhang, C. Cheng, H. Yi, R. Yan, Z. Wu, Y. Wang, X. Shi, G. Yao, G. Zhu and Y. Jia, Efficiently flexo-catalysis driven by bending vibration in amorphous non-piezoelectric nano-SiO_2 for water purification, *J. Alloys Compd.*, 2025, **1014**, 178654.

119 Y. Fu, Z. Xu, H. Liu, R. Fan, W. Tu, W. Xue, X. Zhang, Y. He and D. Gao, Disrupt mitochondrial proton gradients via flexoelectric catalysis to deplete tumor energy and enhance immunotherapy, *Adv. Funct. Mater.*, 2025, **35**, 2421302.

120 A. Li, L. Xu, Y. Jia, M. Yuan, J. Zhang, H. Liu, S. Liu, Y. Zhu, X. Wei, W. Tu, Y. He, S. Ni, X. Jiang and X. Zhang, Flexocatalysis enhances tumor photodynamic therapy, *Small*, 2024, **20**, 2310964.

121 J. Liu, X. Zhou, J. Qian, S. Wang, S. Ma, B. Shen, W. Tu, R. Xu, G. Liu and J. Zhai, Polarization boosted solar H_2O_2 production over quantum dot-decorated nanosheets with rich oxygen vacancies, *ACS Sustainable Chem. Eng.*, 2023, **11**, 18089.

122 A. Kazemi, K. J. Deshmukh, S. Trolier-McKinstry and S. Roundy, Mixed finite element analysis of flexoelectric response: Exploring unit cell stacking and strain gradient

modulation, *arXiv*, 2025, preprint, arXiv:2502.19539, DOI: 10.48550/arXiv.2502.19539.

123 X. Zhuang, B. H. Nguyen, S. S. Nanthakumar, T. Q. Tran, N. Alajlan and T. Rabczuk, Computational modeling of flexoelectricity-a review, *Energies*, 2020, **13**, 1326.

124 P. Wang, B. Q. Liu, X. T. Peng and F. Gao, Bending and vibration behavior of functionally graded piezoelectric nanobeams considering dynamic flexoelectric and surface effects, *Sci. Rep.*, 2025, **15**, 13439.